Insights into Origin and Evolution of α-proteobacterial Gene Transfer Agents

Migun Shakya[1,2], Shannon M. Soucy[1], and Olga Zhaxybayeva[1,3,*]

[1]Department of Biological Sciences, Dartmouth College, Hanover NH 03755, USA

[2]Present address: Bioscience Division, Los Alamos National Laboratory, Los Alamos, NM 87544

[3]Department of Computer Science, Dartmouth College, Hanover NH 03755, USA

*Corresponding author, E-mail: olgazh@dartmouth.edu; Tel: (603) 646-8616

Research Paper

Keywords: exaptation, domestication, horizontal gene transfer, bacterium-virus co-evolution, bacteriophage

Abstract

Several bacterial and archaeal lineages produce nanostructures that morphologically resemble small tailed viruses, but, unlike most viruses, contain apparently random pieces of the host genome. Since these elements can deliver the packaged DNA to other cells, they were dubbed Gene Transfer Agents (GTAs). Because many genes involved in GTA production have viral homologs, it has been hypothesized that GTA ancestor was a virus. Whether GTAs represent an atypical virus, a defective virus, or a virus co-opted by the prokaryotes for some function, remains to be elucidated. To evaluate these possibilities, we examined the distribution and evolutionary histories of genes that encode a GTA in the α-proteobacterium *Rhodobacter capsulatus* (RcGTA). We report that although homologs of many individual RcGTA genes are abundant across bacteria and their viruses, RcGTA-like genomes are mainly found in one subclade of α-proteobacteria. When compared to the viral homologs, genes of the RcGTA-like genomes evolve significantly slower, and do not have higher %A+T nucleotides than their host chromosomes. Moreover, they appear to reside in stable regions of the bacterial chromosomes that are generally conserved across taxonomic orders. These findings argue against RcGTA being an atypical or a defective virus. Our phylogenetic analyses suggest that RcGTA ancestor likely originated in the lineage that gave rise to contemporary α-proteobacterial orders *Rhizobiales, Rhodobacterales, Caulobacterales, Parvularculales, and Sphingomonadales,* and since that time the RcGTA-like element has co-evolved with its host chromosomes. Such evolutionary history is compatible with maintenance of these elements by bacteria due to some selective advantage. As for many other prokaryotic traits, horizontal gene transfer played a substantial role in the evolution of RcGTA-like elements, not only in shaping its genome components within the orders, but also in occasional dissemination of RcGTA-like regions across the orders and even to different bacterial phyla.

1. Introduction

Prokaryotes are hosts not only of their own genetic material, but also of the mobile genetic elements, a broad class of entities that includes integrated viruses (prophages) (Frost et al. 2005). Traditionally, viruses are viewed as selfish genetic elements, but in some instances they can serve as vectors of horizontal gene exchange (HGT) (Touchon et al. 2017), an important driver of evolutionary success of many cellular lifeforms (Koonin 2016; Zhaxybayeva & Doolittle 2011). In other instances, prophage-like elements can provide immunity against other viruses (Canchaya et al. 2003), and therefore are beneficial to their host. While the evolutionary relationship between viruses and cellular lifeforms is still intensely debated, co-option of genes by both empires is likely frequent (Krupovic & Koonin 2017). For example, a few bacteria and archaea encode genes for elements that resemble viral parts and are used for prokaryotic warfare and microbe-animal interactions (Bobay et al. 2014; Borgeaud et al. 2015; Sarris et al. 2014; Shikuma et al. 2014; Touchon et al. 2014). In other instances, viral components appear to have originated from the cellular proteins (Krupovic & Koonin 2017). Such intertwined history of genes from cellular and non-cellular lifeforms resulted in a spectrum of genetic elements that, from the cellular host “point of view”, span from parasitic to benign to beneficial.

One class of such genetic elements is yet to be placed in this spectrum. Several unrelated bacterial and archaeal lineages are observed to produce particles that morphologically resemble viruses, yet appear to carry random pieces of host DNA instead of their own viral genome (Berglund et al. 2009; Bertani 1999; Humphrey et al. 1997; Marrs 1974; Rapp & Wall 1987). These particles were shown to transfer DNA between cells through a transduction-like mechanism (Lang et al. 2012; Mcdaniel et al. 2010), and that’s why they were dubbed “Gene Transfer Agents” (GTAs) (Marrs 1974). Since the transferred DNA may benefit

the recipient cells - for example, it has been proposed that the incoming DNA could be used to repair damaged DNA (Marrs et al. 1977) - GTAs were postulated to be viruses that were "domesticated" by prokaryotes (Bobay et al. 2014) and maintained by them as a mechanism of HGT (Lang et al. 2012). Yet, the details of such co-option event as well as impact of the GTA-mediated HGT remain to be deciphered, and alternatives, such as GTA being instead a defective or atypical virus, need to be evaluated.

The laboratory studies of one of the known GTAs - *Rhodobacter capsulatus*' GTA (or RcGTA for short) - show that this element neither has a typical genome of a bacterial virus nor acts like a typical lysogenic virus. Its genome is distributed across five loci dispersed across the *R. capsulatus* chromosome (Hynes et al. [2016] and **Figure 1A**). Seventeen of the genes are found in a single locus that has a genomic architecture typical of a siphovirus (Lang & Beatty 2007). The majority of the genes in the locus encode structural components of the RcGTA particle (Chen et al. 2009) and are thus referred to as the structural cluster. The remaining four loci contain seven genes shown to be important for RcGTA production, release, and DNA transfer (Fogg et al. 2012; Hynes et al. 2012, 2016; Westbye et al. 2015). Even if RcGTA would preferentially package the regions of DNA that correspond to its own genome, the RcGTA particle head size is too small to fit more than ~1/5 of the genome (Lang et al. 2017), and therefore RcGTA can propagate itself only with the division of the host cell, as a “resident” of the host chromosome. Expression of the RcGTA genes, as well as production and release of RcGTA particles, is known to be triggered by various factors, such as phosphate concentration (Leung et al. 2010; Westbye et al. 2013), salinity (McDaniel et al. 2012), and quorum sensing (Brimacombe et al. 2013; Schaefer et al. 2002). The latter is regulated via CckA-ChpT-CtrA phosphorelay (Leung et al. 2012; Mercer & Lang 2014), one of the widely used signal transduction systems in bacteria that also controls other important cellular functions, such as the cell cycle (Chen & Stephens 2007; Mann et al. 2016) and flagellar motility (Zan et al. 2013).

These observations suggest that RcGTA is under control of the bacterial host and is well-integrated with the host's cellular systems. When did such integration occur? Could RcGTA still represent a selfish genetic element? Based on limited genomic data available at the time, previous studies have inferred that RcGTA-like element was already present in the last common ancestor of all α-proteobacteria (Lang et al. 2002; Lang & Beatty 2007). Through phylogenomic analyses of a much more extensive genomic data set, we show that α-proteobacterial GTA is a virus-related element whose genome evolves differently from what is expected of a typical bacterial virus. We also infer that the RcGTA progenitor was likely absent in the last common ancestor of α-proteobacteria. Instead, we find that RcGTA-like elements are ubiquitous within an α-proteobacterial subclade that gave rise to at least five contemporary taxonomic orders. The phylogenetic histories of RcGTA-like structural cluster genes suggest that the evolution of this element within this subclade was shaped by both vertical descent and HGT.

2. Methods

Detection of RcGTA homologs in viruses and bacteria

Twenty-four genes from the RcGTA genome and its homologs from *Rhodobacterales* were used as queries in BLASTP searches (E-value < 0.001; query and subject overlap by at least 60% of their length) and PSI-BLAST searches (E-value < 0.001; query and subject overlap by at least 40% of their length; maximum of 6 iterations) against viral and bacterial databases using BLAST v2.2.30+ (Altschul et al. 1997). The viral database consisted of 1,783 genomes of dsDNA bacterial viruses extracted from the RefSeq database (release 76; last accessed on July 1, 2016) using "taxid=35237 AND host=bacteria" as a query. Bacterial RefSeq database (release 76; last accessed on June 29, 2016) and 255 completely sequenced α-proteobacterial genomes (**Supplementary Table S1**; genomes downloaded from

ftp://ftp.ncbi.nlm.nih.gov/genomes/Bacteria/ on November 1, 2015) served as two bacterial databases. The detected RefSeq homologs were mapped to their source genomes using "release76.AutonomousProtein2Genomic.gz" file (ftp.ncbi.nlm.nih.gov/refseq/release/release-catalog/, last accessed on June 29, 2016).

Assignment of genes to viral gene families

All annotated protein-coding genes from 255 α-proteobacterial genomes were used as queries in BLASTP searches (E-value < 0.001; query and subject overlap by at least 40% of their length) against the POG (Phage Orhologous Group) database (Kristensen et al. 2013), which was downloaded from ftp://ftp.ncbi.nlm.nih.gov/pub/kristensen/thousandgenomespogs/blastdb/ in February 2016. The genes were assigned to a POG family based on the POG affiliation of the top-scoring BLASTP match.

Identification of RcGTA homologs adjacency in the bacterial genomes

Relative position of RcGTA homologs in the genome was calculated from genome annotations in the GenBank feature tables downloaded from ftp.ncbi.nlm.nih.gov/genomes/all/ on June 29, 2016. Initially, a region of the genome was classified as putative RcGTA-like region if it had at least one RcGTA homolog. The identified regions were merged if two adjacent regions were separated by < 15 open reading frames (ORFs). If the resulting merged region contained at least nine RcGTA homologs, it was designated as a large cluster (LC). The remaining regions were labeled as small clusters (SC).

Examination of viral characteristics of RcGTA-like genes and regions

Prophage-like regions in 255 α-proteobacterial genomes were detected using PhiSpy v2.3 (Akhter et al. 2012) with “-n=5” (at least 5 consecutive prophage genes), “-w=30” (a window size of 30 ORFs), and “-t=0” (“Generic Test Set”) settings. An RcGTA-like region was classified as a putative prophage if it overlapped with a PhiSpy-detected prophage region.

For both large and small clusters, %G+C of the corresponding nucleotide sequence (defined as DNA sequence between the first and last nucleotide of the first and last RcGTA homolog of the region, respectively) was calculated using in-house Python scripts. The relative difference in GC content of the RcGTA-like region and the whole host genome was calculated by taking the difference in their %G+C and dividing it by the %G+C of the host genome. This correction allowed us to compare changes in the GC content of the RcGTA-like regions among genomes with variable GC contents. To account for possible heterogeneity of GC content within each genome, 100 genomic regions of the same size were randomly selected from the genome, their relative GC content calculated as described above and compared to that of the RcGTA-like region(s) using pairwise t-test.

To assess the rate of evolution of RcGTA-like structural genes, pairwise phylogenetic distances (PPD) were examined among RcGTA homologs in viruses, and large and small clusters. The PPDs were calculated using RAxML v8.1.3 (Stamatakis 2014) with PROTGAMMAAUTO option, which selects the best amino acid substitution model and uses Γ distribution with four discrete rate categories to correct for among site rate variation (Yang 1994).

Identification of gene families

Gene families in 255 α-proteobacterial genomes were detected using OrthoMCL v2.0.9 (Li 2003). Specifically, all protein-coding sequences were subjected to all-against-all BLASTP searches (v2.2.30+, E-value < 0.0001), in which reciprocal top-scoring BLASTP matches were retained. The bit scores of the matches were converted to pairwise distances, which were used to form gene families via Markov clustering with the inflation parameter set to 1.2 (van Dongen 2000). The presence/absence of genes in the resulting 33,048 gene families were used to estimate gene family conservation across α-proteobacteria and to characterize the conservation of regions that flank GTA-like regions.

Characterization of immediate gene neighborhoods of small and large clusters

ORFs without detectable similarity to RcGTA genes, but found immediately upstream, downstream, or within structural cluster, were classified based on (a) conservation within α-proteobacterial genomes and (b) potential viral origin. As a proxy for conservation, we used gene family abundance in 255 α-proteobacterial genomes, calculated as the proportion of unique genomes to which an ORF belongs. The ORF was designated as viral if it was assigned to a POG.

Reference phylogeny of α-proteobacteria

From the list of 104 genes families used to reconstruct α-proteobacterial phylogeny (Williams et al. 2007), 99 gene families that are present in 80% of the 255 α-proteobacterial genomes were selected (**Supplementary Table S2**). For each gene family, eight taxa from other groups within *Proteobacteria* were added as outgroup (*Geobacter sulfurreducens* PCA,

Ralstonia solanacearum GMI1000, *Chromobacterium violaceum* ATCC 12472, *Xanthomonas axonopodis* pv citri str 306*, Pseudomonas aeruginosa* PAO1*, Virbrio vulnifucus* YJ016*, Pasteurella multocida* subsp *multocida* str Pm70, *Escherichia coli* str. K12 substr. DH10B). The amino acid sequences of the resulting gene families were aligned using MUSCLE v3.8.31 (Edgar 2004). For each gene family, the best substitution model (listed in **Supplementary Table S2**) was selected using *ProteinModelSelection.pl* script downloaded from http://sco.h-its.org/exelixis/resource/download/software/ProteinModelSelection.pl in August 2016. Additionally, among site rate variation was modeled using Γ distribution with four rate categories (Yang 1994). All gene families were combined into a single dataset with 99 data partitions, one partition per gene family. The maximum likelihood phylogenetic tree was reconstructed in RAxML v8.1.3 (Stamatakis 2014), using the best substitution model for each partition and 20 independent tree space searches. One hundred bootstrap samples were analyzed as described above, and the bootstrap support values > 60% were mapped to the maximum likelihood tree. To obtain reference phylogeny of only LC-containing taxa, the branches corresponding to taxa that have only SCs were pruned from the full reference phylogeny.

Phylogenetic analysis of the large-cluster gene families

Knowing that phylogenetic histories of many RcGTA homologs were poorly resolved in *Rhodobacterales* (Hynes et al. 2016), we combined amino acid sequences of LC gene families into one “LC-locus” dataset in order to increase the number of phylogenetically informative sites. To ensure that such concatenation does not result in a mixture of genes with different evolutionary histories, we compared phylogenetic trees reconstructed from the alignments of individual LC genes and of the concatenated LC-locus. Amino acid sequences of gene families consisting of LC homologs from α-proteobacterial genomes were aligned using MUSCLE v3.8.31 (Edgar 2004). The individual gene family alignments were concatenated into the “LC-

locus" alignment. Since many LCs do not have homologs of all RcGTA structural genes, in the concatenated alignment the absences were designated as missing data (Stamatakis 2014) Additionally, "taxa-matched" LC-locus alignments (*i.e.* concatenated alignments pruned to contain only taxa found in a specific LC gene family) were created. Maximum likelihood trees were reconstructed from the concatenated and individual LC gene alignments, as well as from the taxa-matched LC-locus alignments, using RAxML v.8.2.9 (Stamatakis 2014) under the LG+Γ substitution model (Le & Gascuel 2008; Yang 1994). The LG model was determined as the best substitution model for each individual gene set using the PROTGAMMAAUTO option of RAxML v.8.2.9 (Stamatakis 2014). For each LC gene, consensus trees were reconstructed from 10 bootstrap samples of taxa-matched LC-locus alignments. These consensus trees were compared to 100 bootstrap sample trees for the corresponding LC gene. The congruence between the phylogenies was measured using relative "Tree Certainty All" (TCA) values (Salichos et al. 2014), as implemented in RAxML v.8.2.9 (Stamatakis 2014). The TCA values were classified into three categories: "strongly conflicting" (-1.0 ≤ TCA ≤ -0.7), "moderately conflicting" (-0.7 < TCA < 0.7) and "not conflicting" (0.7 ≤ TCA ≤ 1.0). None of the individual LC gene phylogenies had strongly conflicting TCA values, although 6 out of 17 LC gene phylogenies had moderately conflicting values (**Supplementary Table S3**). Since an uncertain position of just one taxon can affect support values of multiple bipartitions (Aberer et al. 2013) and TCA values calculated from them, we also carried out a Site Specific Placement Bias (SSPB) analysis (Berger et al. 2011), as implemented in RAxML v8.2.9 (Stamatakis 2014). The LC-locus phylogeny and the LC-locus alignment were used as the reference tree and the input sequence alignment, respectively. The sliding window size was set to 100 amino acids. The SSPB analysis revealed that for 15 of the 17 genes only three nodes, on average, separate the optimal positions of each taxon in the gene and LC-locus phylogenies, indicating largely compatible evolutionary histories of individual LC genes and of their combination

(**Supplementary Figure S1**). Consequently, we decided to use the combined, taxa-matched LC-locus alignment for further phylogenetic analyses.

To assess the similarity of the evolutionary histories of LC loci and of their hosts, we compared the topologies of the reference α-proteobacterial tree to 100 bootstrap sample trees reconstructed from the taxa-matched LC-locus alignment assembled as described above. The congruence was quantified using Internode Certainty (IC) values (Salichos et al. 2014), as implemented in RAxML v.8.2.9 (Stamatakis 2014). Similar to the TCA value classification, the IC values were classified into three categories: “strongly conflicting” ($-1.0 \leq IC \leq -0.7$), “moderately conflicting” ($-0.7 < IC < 0.7$) and “not conflicting” ($0.7 \leq IC \leq 1.0$).

Conservation of gene neighborhoods across phylogenetic distance

Forty ORFs upstream and downstream of ATP synthase operon, ribosomal protein operon, and LCs were extracted from 87 α-proteobacterial genomes that contain at least one LC. The same procedure was performed for a transposase from IS3/IS911 family, which was detected in 18 of the 87 genomes. Each ORF was assigned to a gene family, and the pairwise conservation of the corresponding flanking regions was calculated as a proportion of gene families shared between two genomes. PPDs of 16S rRNA genes were used as a proxy for time *t*. 16S rRNA genes were aligned against the GreenGenes database (Desantis et al. 2006) (last accessed in August 2016) using mothur v.1.35.1 (Schloss et al. 2009). The PPDs were calculated from the alignment using RAxML v8.1.3 (Stamatakis 2014) under GTR+Γ substitution model. Based on *model 3* from (Rocha 2006), the gene neighborhood decay was modeled as p^t, where p is the probability of the 40 ORFs to remain in the same genomic region and t is time. This model assumes that every gene has equal probability of separating from the region. The

parameter *p* was estimated, and the fit between the model and data was assessed using non-linear least squares method (Bates & Watts 1988), as implemented in the *nls* R function.

Examination of genes that flank RcGTA-like clusters in non-α-proteobacterial genomes

Amino acid sequences of five ORFs upstream and downstream of the RcGTA-like clusters in the genomes of actinobacteria *Streptomyces purpurogeneiscleroticus* NRRL B-2952 (GenBank accession number LGEI00000000.1;(Ju et al. 2015)) and *Asanoa ferruginea* NRRL B-16430 (LGEJ00000000.1; (Ju et al. 2015)), a γ-proteobacterium *Pseudomonas bauzanensis* W13Z2 (JFHS00000000.1; (Wang et al. 2014)), and a cyanobacterium *Scytonema millei* VB511283 (JTJC00000000.1; (Sen et al. 2015)) were searched against the database of protein-coding genes of 255 α-proteobacterial genomes using BLASTP (E-value < 0.001; query and subject overlap by at least 60% of their length). In *P. bauzanensis* and *S. millei* three genes (*kpdE*, *pbpC*, *dnaJ*) were found to share similarity with genes observed near RcGTA-like regions in α-proteobacteria. To examine evolutionary histories of these three genes, their homologs from other cyanobacteria and γ-proteobacteria were identified by BLASTP searches of γ-proteobacteria and cyanobacteria present in the *nr* database (https://blast.ncbi.nlm.nih.gov/Blast.cgi, last accessed on October 31, 2016; E-value < 0.001; query and subject overlap by at least 60% of their length) using KpdE, PbpC, DnaJ homologs from *P. bauzanensis*, *S. millei* and α-proteobacteria as queries. For each of the three gene sets, four homologs from each identified taxonomic group were selected and combined with all available homologs from LC-containing α-proteobacteria. The amino acid sequences of the combined data sets were aligned using MUSCLE v3.8.31 (Edgar 2004). Maximum likelihood trees were reconstructed using FastTree v2.1.8 (Price et al. 2010) under JTT+Γ substitution model. The trees were visualized and annotated using EvolView (He et al. 2016)

(http://evolgenius.info/evolview, last accessed on November 13, 2016).

Identification of CRISPR/*Cas* defense systems

Spacers of the Clustered Regularly Interspaced Short Palindromic Repeats (CRISPRs) were identified by scanning 255 α-proteobacterial genomes for both CRISPR leader sequences and repeat structures using CRISPRleader v1.0.2 (Alkhnbashi et al. 2016) and PILER-CR v1.06 (repeat length between 16 and 64; spacer length between 8 and 64; minimum array length of 3 repeats; minimum conservation of repeats 0.9; minimum repeat length ratio 0.9; minimum spacer length ratio 0.75) (Edgar 2007), respectively. Additionally, CRISPR-associated proteins were identified by searching protein-coding gene annotations for the presence of the words "CRISPR" or "Cas" in combination with *Cas* family annotations from (Makarova et al. 2015). Genomes were designated to have putative functional CRISPR/*Cas* systems if both CRISPR spacer arrays and CRISPR-associated proteins were present. Spacer sequences from these putatively functional CRISPR systems were used as BLASTN (v.2.4.0+; E-value<10; task = tblastn-short) queries against all gene sequences in LCs.

Identification of decaying RcGTA structural cluster homologs

The nucleotide sequences of LC and SC regions were extracted from each genome and translated in their entirety into all six reading frames. RcGTA structural cluster genes were used as BLASTP (v2.4.0+, e-value ≤ 0.001) queries in searches against the database of translated LC and SC regions. Homologous sequences within LC and SC regions that did not match the annotated ORFs were designated as putatively decaying RcGTA genes.

3. Results

Many RcGTA genes share evolutionary history with viruses

Consistent with the earlier proposed hypothesis that RcGTA is an element originated from a virus (Lang & Beatty 2000), 14 out of 24 RcGTA genes can be assigned to a viral gene family (Phage Orthologous Group, or POG; Kristensen et al. 2013) (**Figure 1A** and **Supplementary Table S4**), and 18 out of the 24 genes have at least one detectable homolog in available genomes of *bona fide* bacterial viruses (**Figure 1B**). However, at the time of our analyses none of the contemporary bacterial viruses available in RefSeq database contained a substantial number of the RcGTA homologs (at most eight of them in *Rhizobium* phage 16-3 [GenBank Acc. No. DQ500118.1]), and no α−proteobacterial genomes with CRISPR systems contained significant matches between CRISPR spacers and RcGTA genome, suggesting that the presumed progenitor virus is either extinct or remains unsampled. Collectively, RcGTA-like genes are unevenly represented across viral genomes (**Figure 1B**). Among the five most abundant are homologs of *rcc001683* (*g2*), *rcc001684* (*g3*), *rcc001686* (*g4*) and *rcc001687* (*g5*) genes, which encode terminase, portal protein, prohead protease, and major capsid protein, respectively, all of which are of HK97-like types. Such widespread occurrence of these structural cluster genes is not surprising. First, these genes correspond to the so-called “viral hallmark genes”, defined as genome replication and virion formation genes with a wide distribution among diverse viral genomes (Iranzo et al. 2016; Koonin et al. 2006). Second, HK97-like homologs of these genes are commonly used among known Caudovirales (Iranzo et al. 2017), one of the most abundant group of viruses on Earth (Cobián Güemes et al. 2016). However, 13 of the RcGTA genes are either sparsely represented (found in 10 or fewer viral genomes; 7 genes) or not detected at all (6 genes) in viruses. These genes may be fast-

evolving viral genes, auxiliary (non-hallmark) viral genes, which could be specific to the viral lineage that gave rise to RcGTA, non-viral (cellular) genes, or simply be a result of undetected homology due to the paucity of viral genomes in GenBank. The latter possibility cannot be ignored, especially given that (i) three of the 13 genes are assigned to a POG category (**Figure 1A**), and therefore are likely of viral origin, and (ii) only 94 of the 1,783 screened bacterial viruses (5%) have α-proteobacteria as their known host. Since about half of bacterial genomes are estimated to contain at least one prophage in their genome (Touchon et al. 2016), inclusion of RcGTA homologs from bacterial genomes could reduce the possibility of undetected homology due to lack of available viral genomes. Therefore, we looked for RcGTA homologs in all bacterial RefSeq records, and in 255 completely sequenced α-proteobacterial genomes in particular (**Supplementary Table S1**).

Homologs of RcGTA genes are abundant in bacteria, but RcGTA-like genomes are mainly found in class α-proteobacteria

Every RcGTA gene has at least 198 homologs in RefSeq database (**Figure 1C**), and therefore even the 13 “rare” genes are relatively abundant in bacterial genomes. Moreover, six of the 13 genes (*rcc00171*, *rcc00556*, *rcc01688* (*g6*), *rcc01692* (*g10*), *rcc001695 (g12),* and *rcc01866*), including three assigned to POGs, are found in more than 1000 bacterial genomes (**Figure 1C**). Therefore, it is unlikely that the 13 rare genes are auxiliary viral genes specific to the viral lineage that gave rise to RcGTA. However, only future availability of a larger number of genomes of α-proteobacterial viruses will help identify if these genes are of viral or cellular origin.

Collectively, detected bacterial homologs of RcGTA genes are found in organisms within 13 phyla (**Figure 1C** and **Supplementary Figure S2a**). Interestingly, 84% and 35% of the identified homologs belong to the phylum Proteobacteria and to its class α-proteobacteria,

respectively (**Supplementary Figure S2**). Furthermore, in many α-proteobacteria there are more RcGTA homologs per genome than in any available viral genome, and these homologs are often clustered (**Supplementary Figure S2b**). In contrast, most other taxa have only few RcGTA homologs that are scattered across the genome (**Supplementary Figures S2b** and **S2c**). Given that in the RcGTA genome, the structural genes are in one locus (**Figure 1A**) and are presumed to be co-transcribed (Kuchinski et al. 2016), our observations suggest that functional GTAs might be restricted mainly to α-proteobacteria.

Within α-proteobacteria, homologs of RcGTA genes are detectable in 197 out of 255 examined genomes (77%). These homologs are distributed across eight α-proteobacterial orders with at least one available genome and two unclassified α-proteobacterial genera (**Figure 2**). While the majority (13 out of 17) of the genes from the RcGTA structural cluster locus are abundant across α-proteobacteria (and across Bacteria in general), only two of the genes from the remaining four loci (*rcc00555* and *rcc01866*) are frequently detected in bacterial genomes (**Figure 1C** and **Figure 2**), which is also consistent with an earlier observation that most of the RcGTA genes outside of structural cluster evolve faster than their structural counterparts in *Rhodobacterales* (Hynes et al. 2016). Therefore, for the subsequent investigations we focused mostly on the analyses of the gene from the structural cluster locus.

Two distinct classes of RcGTA structural cluster homologs are present in α-*proteobacteria*

Within 187 α-proteobacterial genomes with at least one structural cluster homolog, the RcGTA-like genes are dispersed across 474 genomic regions, more than half of which (245) have only one or two RcGTA homologs (**Figure 3**). Due to significant similarity of a few of RcGTA structural genes to the widely used HK97-like counterparts (Iranzo et al. 2016), some of

these regions may belong to prophages unrelated to RcGTA. Indeed, 261 out of 474 regions (55%) overlap with putative prophages identified using PhiSpy (Akhter et al. 2012) (**Supplementary Figure S3**). However, PhiSpy predictions are likely to include false positives, since the RcGTA itself is classified by PhiSpy as a prophage. Also, the remaining 213 RcGTA-like regions could contain false negatives, given the small size of many RcGTA-like genomic regions (and presumably of related viruses) and a PhiSpy prophage assignment requirement for presence of at least five consecutive genes with "viral" functional annotations in a window of 30 genes. Therefore, we examined the RcGTA-like regions and genes within them for additional characteristics associated with viral genes – skewed nucleotide composition (Rocha & Danchin 2002) and faster substitution rates (Drake 1999; Paterson et al. 2010) – as well as the presence of neighboring viral genes.

Genes of viral origin generally have lower fraction of Gs and Cs (GC content) than their host genomes (Rocha & Danchin 2002). Interestingly, we do not observe this trend for the RcGTA-like regions. GC content of the regions with less than nine RcGTA homologs (hereafter referred as small clusters, or SC) is, on average, equivalent to the GC content in the host (median of percent of relative change = -0.1%; pairwise Wilcoxon test; *p*-value=0.60), albeit with substantial variability across examined genomes (**Figure 4**). On the other hand, GC content of the regions with at least nine RcGTA homologs (hereafter referred as large clusters, or LC) is consistently, and in most cases significantly higher than the GC content of their host (median of percent of relative change = 6.57%; pairwise *t* test; *p*-value < 0.001) (**Figure 4**). The elevated GC content of LCs also persists when compared to randomly sampled regions of the host genome of equivalent size (pairwise t-test; *p-value* <0.001). The observed differences in the relative GC content between RcGTA genes in large and small clusters prompted us to examine the features of these two categories of RcGTA-like genomic regions separately.

Using the pairwise phylogenetic distances (PPD) of these genes as a proxy for substitution rates, we found that LC genes have significantly lower PPDs than both their SC (all

of the 13 possible pairwise comparisons; Wilcoxon tests; *p*-values <0.0001) and viral homologs (14 out of 15 possible comparisons; Wilcoxon tests; *p*-values <0.005) (**Supplementary Figure S4** and **Supplementary Table S5**). And while many SC genes also have significantly lower PPDs than their counterparts in viral genomes (six out of 10 possible comparisons; Wilcoxon tests; *P*-values <0.005), the 25-75 percentile range for PPDs of SC genes often overlapped with that of the viral homologs (**Supplementary Figure S4**). These data suggest that large and small clusters evolve at different rates, with SCs appearing more virus-like. In support of this conjecture, SCs are more frequently associated with unrelated viral genes than LCs (76 vs. 56%; **Supplementary Figure S3**). For example, in order *Rhodospirillales* all but two SCs are near such viral genes (**Supplementary Figure S3**). In other cases, SCs likely belong to viral elements that are clearly not GTAs: for example, in all analyzed genomes of the *Rickettsiales'* genera *Anaplasma* and *Ehrlichia* a singleton homolog of *rcc001695* (g12) is found within 1Kb of *vir*B homologs, which in *Anaplasma phagocytophilum* are part of a virus-derived type IV secretion system (Al-Khedery et al. 2012). Furthermore, SCs have very little conservation of flanking genes (**Supplementary Figure S5)**, while in LCs flanking genes are conserved within orders and sometimes even across larger phylogenetic distances (**Supplementary Figure S6)**.

Nevertheless, small size and faster evolutionary rates of some SCs may instead be indicative of a decay of the previously functional GTAs. While bacterial genomes do not generally contain many pseudogenes due to genome streamlining (Lawrence et al. 2001), if remnants of RcGTA homologs that no longer form an ORF remain within the regions, they may still be detectable by similarity searches of genomes. Such searches revealed that putative pseudogenes of RcGTA-like genes are indeed detectable in both large and small clusters, although 65% of them are found in LCs (**Supplementary Figures S2, S5** and **S6**).

Taken together, we suggest that large and small clusters of RcGTA-like genes represent genomic regions that are under different selective pressures in the host chromosome and may have separate evolutionary histories. This distinction is not captured in the PhiSpy-based

classification of viral elements. We further hypothesize that most SCs are viral elements unrelated to RcGTA and may not be GTAs at all. On the other hand, LCs appear to evolve in a manner expected from a genetic element that has resided with its host chromosome for a prolonged time, and therefore we conclude that only LCs represent RcGTA-like elements. In what lineage did the RcGTA-like element originate? How did it propagate across α-proteobacteria? To address these questions, we examined the phylogenetic history of LCs in the α-proteobacteria.

RcGTA-like element was likely absent in the last common ancestor of α-*proteobacteria*

Within α-proteobacteria, LCs are found only within a monophyletic clade defined by node 1 in **Figure 5** (hereafter referred as Clade 1), which consists of all included representatives from the orders *Rhizobiales, Caulobacterales*, *Rhodobacterales, Parvularculales* and *Sphingomonadales*. Two deeper branching α-proteobacterial clades that include *Rickettsiales*, *Rhodospirillales,* and yet unclassified *Micavibrio* spp. and SAR 116 cluster bacteria contain only SCs (**Figure 5**), the largest of which is made up of five genes, but most are singletons (**Figures 2** and **3**). RcGTA homologs (including genes outside of the structural cluster) are completely absent from *Pelagibacterales* (formerly SAR11) and the basal α-proteobacterial order *Magnetococcales* (**Figure 5**), although only five genomes from these two groups were available for the analyses. Moreover, only 3 of 199 SCs found in taxa outside of Clade 1 contain detectable putative pseudogenes of the RcGTA structural genes (**Supplementary Figure 3**). Taking into account the observation that the fraction of genomes with no detectable RcGTA homologs is higher in taxa outside than inside of Clade 1 - 30% versus 15% of the genomes, respectively, - we hypothesize that the RcGTA-like element did not originate in the last common ancestor of α-proteobacteria (Clade 2 in **Figure 5**), as was previously suggested (Lang & Beatty

2007). Instead, we propose that the RcGTA-like element appeared later in the evolution of α-proteobacteria, either on the branch leading to the last common ancestor of Clade 1, or later within Clade 1. In the former case, the element would have passed vertically as the lineages diverged, while in the latter scenario it would have spread across Clade 1 via HGT. To evaluate these two scenarios, we performed additional phylogenetic analyses.

Evolution of the RcGTA-like genome: Vertically Inherited or Horizontally Exchanged?

Earlier examination of the RcGTA structural cluster genes' evolutionary histories concluded that RcGTA-like element had evolved vertically within α-proteobacteria *(Lang & Beatty 2007)*, although only few genomes were available at the time. A more recent phylogenetic analysis of RcGTA-like clusters within order *Rhodobacterales* was also compatible with the vertical inheritance of the RcGTA structural cluster genes within the order, although phylogenetic histories of many individual RcGTA genes were poorly resolved (Hynes et al. 2016). Nevertheless, there is accumulating evidence that individual RcGTA-like genes, and even whole structural clusters, may have been at least occasionally horizontally exchanged. For example, RcGTA-like genes involved in recipient cell recognition (especially homologs of *rcc00171*) are presumed to be horizontally exchanged within *Rhodobacterales* (Hynes et al. 2016). Additionally, while LCs are predominantly found in α-proteobacteria, the genomes of the actinobacteria *Streptomyces purpurogeneiscleroticus* NRRL B-2952 and *Asanoa ferruginea* NRRL B-16430, the cyanobacterium *Scytonema meliloti* VB511283, and the γ-proteobacterium *Pseudomonas bauzanensis* W13Z2 also contain one LC each (**Supplementary Figures S2** and **S6**). To investigate the extent of HGT in the evolution of the RcGTA-like genes in Clade 1, we reconstructed the phylogeny of the LC-locus (see **Methods** for details about its construction) and compared it to the reference tree of α-proteobacteria, with the latter represented by a set of

conserved α-proteobacterial genes.

Although LC locus appears to evolve ~ 1.6 times faster than the conserved 99 α−proteobacterial genes, with a few exceptions, the phylogeny of the LC locus reflects the reference phylogeny arrangement of taxonomic groups at the order and family levels (**Figure 6**). However, 42 out of 83 internal branches of the reference phylogeny are in conflict with the branching order of the LC-locus phylogeny, suggesting that some HGT has taken place. Thirty-one of the 42 conflicts (74%) are within taxonomic orders, with the 14 out of 21 *strongly* supported conflicts limited to genera (**Figure 6** and **Supplementary Figure S7**). Among the nine conflicts at deep branches, eight are due to an alternative position of *Methylobacterium nodulans* ORS 2060 (**Figure 6** and **Supplementary Figure S7**), which, in addition to grouping outside of its order *Rhizobiales,* has five non-identical LCs (**Supplementary Figure S6**). Therefore, most HGT events have likely occurred between closely related taxa.

Intriguingly, at least occasionally LCs have also been transferred across *very large* evolutionary distances: the four non-α-proteobacterial, LC-containing taxa mentioned above branch within the Clade 1, in three separate locations (**Figure 6**), indicating that these taxa most likely acquired the LCs from the α-proteobacteria at least three times independently. Moreover, the LCs of two of the four taxa (the cyanobacterium *Scytonema millei* and the γ-proteobacterium *Pseudomonas bauzanensis*) are flanked by the genes homologous to the genes that flank LCs in their respective α-proteobacterial sister taxa (**Supplementary Figure S6**). Phylogenetic analyses revealed that *S. millei*'s and *P. bauzanensis*' flanking genes are also of α-proteobacterial origin (**Supplementary Figure S8**), and hence were likely acquired in the same HGT events.

Additional clues about the duration of the association of RcGTA-like elements with bacterial genomes could be obtained by investigating the stability of the host chromosome regions that surround LCs, which can be evaluated by examination of conservation of genes upstream and downstream of large clusters across phylogenetic distance (gene synteny). For

example, very dynamic genomic regions known as genomic islands exhibit poor gene synteny even across short phylogenetic distances (Rodriguez-Valera et al. 2016). Highly mobile genes, such as transposable elements and some prophages, are often found in such genomic islands (Juhas et al. 2009). On the other hand, gene synteny of stable regions is preserved across larger evolutionary distances, although it is still subject to decay due to rearrangements that are not due to HGT (Brilli et al. 2013; Rocha 2006). Interestingly, LCs found in the same taxonomic order are generally flanked by the same, conserved α-proteobacterial genes (**Supplementary Figure S6**), hinting that they might be part of stable regions of bacterial chromosomes and not within genomic islands. To more comprehensively evaluate the stability of the genomic region surrounding the LC loci, we modeled gene order decay as a function of phylogenetic distance (Rocha 2006) and compared the conservation of genes flanking LCs to that of a transposable element from IS911/IS3 family and two operons of conserved housekeeping genes, the ribosomal protein operon and the ATP synthase operon. The transposable element from IS911/IS3 family can undergo non-targeted integration (Chandler et al. 2015), and thus, genes adjoining these transposons are not expected to be homologous even across closely related taxa, while gene order near presumably non-mobile housekeeping operons are expected to be much more conserved across time. Indeed, we found that the regions surrounding the transposable element are too variable to even fit the model (**Supplementary Figure S9**). On the other hand, the decay of gene synteny near LCs is similar to that of the two operons (**Supplementary Figure S9**). Therefore, it is unlikely that RcGTA-like elements reside in dynamic regions of their host genomes.

In contrast to the evolutionary history of the structural cluster locus, the remaining four loci of the RcGTA genome are poorly conserved across the genomes of Clade 1 (**Figure 2**), and, within *Rhodobacterales*, one of these loci (consisting of just one *rcc00171*-like gene that encodes tail fiber protein) was likely recently acquired from a viral donor (Hynes et al. 2016). These observations raise a possibility the RcGTA progenitor genome may not have contained

the loci outside of the structural cluster and instead they were recruited later via HGT. Poor conservation of the genes from the four loci across large evolutionary distances (**Figure 1** and **Figure 2**) makes it difficult to test this hypothesis. Intriguingly, in 66 α-proteobacterial genomes that contained two of the readily detectable genes (homologs of *rcc00171* and *rcc00555*), 22 LCs from Rhizobiales and Rhodobacterales have *rcc00171* homologs at their 3' end (**Supplementary Figure S6**). Moreover, 6 of the 22 LCs additionally have *rcc00555* at the 3' end. This anecdotal evidence suggests that in the past RcGTA-like elements may have carried at least some of the genes in one locus with the structural cluster genes, and that the division of the GTA genome into multiple loci may have happened after the bacterium-GTA association was already established.

Taken together, our analyses suggest a complex evolutionary history of the locus. The congruence of both the reference and the LC-locus phylogenies at taxonomic order and family levels and conservation of LC-flanking genes within orders suggest that RcGTA-like element was likely acquired before the contemporary orders within Clade 1 have diversified, and since that time the element co-existed with the clade members. The congruence with the reference phylogeny, however, does not necessarily means that this long-term association is due to vertical inheritance, given that even genes highly conserved across α-proteobacteria are not immune to HGT and thus the reference phylogeny may not represent the strictly vertical history of α-proteobacteria (Gogarten et al. 2002; Andam et al. 2010). Indeed, strong phylogenetic conflicts between the reference and LC locus phylogenies of Clade 1 at both deep and shallow branches, and presence of LCs in multiple taxa outside of the α-proteobacteria indicate that HGT has been shaping the evolution of RcGTA-like element to a non-negligible degree. Since the majority of the strongly supported conflicts are found within genera, HGT probably played a larger role in the recent evolution of RcGTA-like elements than in their dissemination across Clade 1.

4. Discussion

Many prokaryotic cellular functions that are associated with adaptations, such as cell-cell warfare, microbe-animal interactions, HGT and response to environmental stress, are carried out using structures that resemble viral “heads” (e.g. McHugh et al. 2014; Sutter et al. 2008) or “tails” (e.g. Borgeaud et al. 2015; Shikuma et al. 2014), and appear to be widespread across archaea and bacteria (e.g. Böck et al. 2017; Sarris et al. 2014). The prevailing hypothesis is that these elements are examples of exaptations of viral parts via “domestication” of previously purely selfish (viral) elements by prokaryotes (Bobay et al. 2014; Touchon et al. 2014). Do GTAs represent such a case of virus domestication? For how long do such elements persist in microbial genomes? Our survey of RcGTA homologs in the genomes of bacteria and bacterial viruses provide new insights into fascinatingly intertwined evolutionary histories of some viruses and their bacterial hosts.

Although we infer that the RcGTA-like element is not as ancient as the class α-proteobacteria itself (as was proposed in Lang & Beatty 2007), we found that RcGTA homologs are ubiquitous across an α-proteobacterial clade that spans multiple α-proteobacterial orders (Clade 1 in **Figure 5**) and, according to molecular clock estimates, has originated between 777 Mya (Luo et al. 2013) and 1710 Mya (with a 95% CI of 1977-1402 Ma; Gregory Fournier, pers. comm.) Therefore, either RcGTA-like element has been associated with a group of α-proteobacteria for hundreds of millions of years, or it is a vestige of a very successful virus capable of inter-species and inter-order infections. The latter scenario is supported by experimentally observed long-range HGT via GTAs produced by *Roseovirus nubinhibens* ISM (McDaniel et al. 2010). However, our findings of lack of CRISPR repeats that match RcGTA genome, absence of closely-related contemporary viruses in GenBank, and order-level congruence of the evolutionary histories of RcGTA and conserved α-proteobacterial genes point against the GTA being derived from a broad host-range virus that recently invaded this clade.

Instead, our data are more compatible with a long-term association between a GTA and its bacterial host.

Over this time, the GTA genome has gone through extensive changes, as hinted by the putative HGT events within taxonomic orders, presence of likely pseudogenized RcGTA homologs within a few putative GTAs, and division of the RcGTA genome into multiple loci. Could these modifications simply mean that this RcGTA-like element is just a defective prophage (Redfield 2001; Solioz & Marrs 1977) not yet purged from the genomes? Since bacterial genomes are generally under deletion bias of unnecessary DNA (Mira et al. 2001), conservation of “junk” regions across over millions of years is unexpected. Moreover, given the universal mutation bias towards AT-rich DNA (Hershberg & Petrov 2010), over such prolonged time we would expect the defective prophage region to become more AT-rich than the host DNA, and to accumulate mutations evenly across non-synonymous and synonymous sites of the decaying ORFs (Andersson & Andersson 2001). Yet, at least across *Rhodobacterales*, RcGTA homologs do not exhibit increased rates of non-synonymous substitutions expected of pseudogenes (Lang et al. 2012), and compositionally genomic regions that encode LCs are not AT-richer than the rest of the host chromosomes, suggesting that LCs are unlikely to be decaying prophages.

Surprisingly, RcGTA-like gene clusters have a significantly elevated % G+C than chromosomes of their hosts. Evolution of GC content and its variation across the prokaryotic genomes is an unsolved puzzle, with many possibilities invoked to explain it (Hildebrand et al. 2010; Lassalle et al. 2015; Rocha & Feil 2010). Intriguingly, there is a negative correlation between a GC content of a gene and its expression level, with a possible explanation that highly expressed genes tend to be AT-rich due to their accumulation of mutations during the single-stranded DNA state required for transcription (Hildebrand et al. 2010). Since, evolutionarily speaking, the structural cluster locus is never expressed (RcGTA-producing cells lyse and thus leave no progeny), it is tempting to speculate that selection for reduced gene expression may

have played a role in driving the GC content of the structural locus higher than that of the expressed host genes. Future testing of this hypothesis and exploring other possible explanations are necessary to account for the aberrant GC content of the RcGTA-like regions within Clade 1 genomes.

But if RcGTA-like elements are indeed functional, why do we observe putatively pseudogenized and apparently incomplete gene repertoires of many LCs when compared to the RcGTA genome? Perhaps, genomes of these elements are also split into different pieces, have some components replaced from sources unrelated to the RcGTA, or have evolved to a different functionality than RcGTA. For example, GTA gene expression and GTA particle release was demonstrated for *Ruegeria pomeroyi* DSS-3 (Biers et al. 2008) and *Rhodovulum sulfidophilum* (Nagao et al. 2015), suggesting that GTA is functional in these lineages. However, the *R. pomeroyi* and *R. sulfidophilum* genome contain no detectable homologs of *g1*, although this gene is essential for RcGTA production in *R. capsulatus* (Hynes et al. 2016). Therefore, even presumably “incomplete” LCs may encode functional GTAs. The functionality of the identified putative GTAs in the contemporary Clade 1 taxa awaits experimental demonstration.

With the evidence pointing against the *decaying* or a *selfish* nature of the RcGTA-like elements, and given that cells that produce RcGTA lyse (Westbye et al. 2013) and, therefore, the selection for the maintenance of RcGTA cannot occur at a level of an organism, earlier suggestions that GTA maintenance is due to some *population*-level benefits (Lang et al. 2012) remain most plausible explanation of persistence of RcGTA-like elements in the Clade 1 genomes. However, specific advantage(s) associated with acquisition of ~4kb pieces of random DNA via GTA remain to be elucidated. Among the proposed drivers of GTA maintenance are effective exchange of useful genes among the population of heterogeneous cells (Smillie et al. 2011) and improved response to environmental stressors, such as DNA damage (Brimacombe et al. 2015) and nutritional deficits (Lang et al. 2012). Possibilities unrelated to GTA-mediated DNA delivery, such as protection of the host population against infection by other viruses via the

superinfection immunity mechanism (Díaz-Muñoz 2017), and increase of the host population resilience against various environmental stressors such as antibiotics (Wang et al. 2010), should also be considered. Perhaps, there is no single benefit associated with RcGTA-like elements across all Clade 1 taxa. Instead, different lineages may experience selection pressures unique to their ecological niches.

Interestingly, GTA-associated benefits have been proposed to drive evolutionary innovations of cellular lifeforms that go beyond population level. For example, it has been hypothesized that abundance and mixed ancestry of α−proteobacterial genes in eukaryotic genomes is due to the delivery of such genes by RcGTA-like elements into proto-eukaryote genome, and that such "seeding" facilitated the later integration of mitochondrial progenitor and the proto-eukaryotic host (Richards & Archibald 2011). Our study, however, does not support this hypothesis. First, based on the estimated age of the Clade 1 (777-1710 Mya) and the appearance of eukaryotic, and hence mitochondria-containing, organisms in the fossil record (1600 and possibly 1800 Mya; Knoll 2014), the RcGTA-like system likely originated after the eukaryogenesis took place. Second, α-proteobacterial lineage(s) suggested to have given rise to mitochondrial progenitor (Brindefalk et al. 2011; Thrash et al. 2011; Wang & Wu 2015) appear to lack LCs and therefore unlikely to have had RcGTA-like elements. In another intriguing hypothesis, an unrelated GTA in *Bartonella* has been proposed to have facilitated adaptive radiation within the genus (Guy et al. 2013). Perhaps, acquisition of the RcGTA-like element by the last common ancestor of Clade 1 taxa represent a similar innovation that led to diversification of this clade and success of its members in a variety of ecological settings that span soil, freshwater, marine, waste water, wetland and eukaryotic intracellular environments.

Despite the appearance that bacteria maintain GTA genes for the potential contribution to their own evolutionary success, there is an undeniable shared evolutionary history between RcGTA-like elements and *bona fide* viruses. Presence of homologs for most RcGTA-like genes in *bona fide* viral genomes, as well as similarity in the organization of the structural cluster and

corresponding region of a typical siphovirus genome (Huang et al. 2011), led to a prevailing hypothesis that RcGTA originated in an initial co-option of a virus and evolved in subsequent modification of the progenitor prophage genome via vertical descent and HGT (Lang et al. 2017). Our data are compatible with this scenario, and further suggest an even larger role of HGT in the evolution of RcGTA-like elements than currently acknowledged, shaping GTAs both within α−proteobacterial orders, but also at least occasionally transferring RcGTA-like regions across the higher-order α−proteobacterial taxa and even to different phyla. Yet, there are hints of even more entangled connection between RcGTA-like genes found in cellular and viral genomes: a few viruses that infect *Paracoccus*, *Roseobacter*, *Caulobacter*, and *Rhodobacter* spp., and a yet unclassified marine Rhizobiales str. JL001 bacterium, carry RcGTA-like genes that are phylogenetically placed within their cellular homologs (Zhan et al. 2016), suggesting that some viruses acquired genes from the cellular RcGTA-like regions. Given recent propositions of (*i*) cellular origin of even such “hallmark” viral genes like those encoding capsid proteins (Krupovic & Koonin 2017), (*ii*) the possibly virus-independent origin of cellular microcompartments that resemble viral structures (Bobik et al. 2015), and (*iii*) the potentially primordial origin of type VI secretion system that resembles a bacteriophage tail (Böck et al. 2017), we should not exclude a possibility that genomic regions encoding RcGTA-like nanostructures did not originate by a co-option of a prophage and its subsequent modification, but instead are a mosaic originally assembled within bacterial genomes from the available cellular and viral parts.

Acknowledgements

We would like to thank Andrew S. Lang, J. Thomas Beatty and Rosemary J. Redfield for numerous stimulating discussions regarding GTA evolution.

Conflict of Interest: None declared

Funding

This work was supported by the National Science Foundation (NSF-DEB 1551674 to O.Z.); the Simons Foundation (Investigator in Mathematical Modeling of Living Systems award 327936 to O.Z.); the Neukom Institute CompX award to O.Z.; and Dartmouth start-up funds to O.Z.

Author Contributions

MS and OZ designed the study. MS and SMS performed the analyses. MS, SMS, and OZ wrote the manuscript. All authors have seen and approved the final manuscript.

Data Availability

Amino acid sequences of RcGTA homologs in bacterial and viral genomes; amino acid sequence alignments of RcGTA homologs from the LCs, SCs, and viruses; concatenated alignment of 99 conserved α-proteobacterial genes and RcGTA homologs from LCs; and discussed phylogenetic trees in Newick format are available via FigShare at DOI 10.6084/m9.figshare.5406733.

Figure Legends

Figure 1

RcGTA genome and distribution of its homologs in viral and bacterial genomes. Panel A. The RcGTA genome architecture. The RcGTA genome consists of 24 genes scattered across five loci in the *R. capsulatus* SB1003 genome. The genes are represented by arrows, which are drawn to scale, and are labeled using *R. capsulatus* SB1003 locus tags. The majority of the structural cluster genes (*rcc01682-rcc01698*; also known as *g1-g15*) encode structural components of the RcGTA particle (Chen et al. 2009), *rcc00171* (*tsp*) encodes a tail spike protein (Hynes et al. 2016), *rcc00555* and *rcc00556* - endolysin and holin (Fogg et al. 2012; Hynes et al. 2012; Westbye et al. 2013), *rcc01079* (*ghsA*) and *rcc01080* (*ghsB*) - encodes a head spike (Westbye et al. 2015), and *rcc01865* and *rcc01866* - putative regulatory elements (Hynes et al. 2016). The full GenBank functional annotations of the genes are listed in **Supplementary Table S4**. Genes with similarity to gene families in the POG database (Kristensen et al. 2013) are shaded and their assigned POG categories are listed in **Supplementary Table S4. Panel B. Presence of RcGTA gene homologs in 1,783 viral genomes.** The numbers above arrows represent the total number of detected homologs for each RcGTA gene, while the percent of viral genomes in which these homologs are found is depicted in shades of gray (see figure inset for scale). **Panel C. Presence of RcGTA gene homologs in 30,503 bacterial genomes.** The numbers above arrows represent the total number of detected homologs for each RcGTA gene, while the percent of bacterial genomes in which these homologs are found is depicted in white and various shades of gray (see figure inset for scale). Genomic regions were visualized using R package genoplotR (Guy et al. 2010).

Figure 2

Presence of RcGTA-like genes in α-proteobacterial genomes. The homologs of the structural cluster genes are found in 184 genomes spanning eight out of ten α-proteobacterial orders with at least one available genome, and in three genomes within two α-proteobacterial genera, *Micavibrio* and *Polymorphum*, which are unclassified at the order level. The homologs of the RcGTA genes from the other four loci are detected in 109 of the 187 genomes spanning six α-proteobacterial orders and one unclassified taxon. Each line represents the distribution of genes in the RcGTA genome within each taxonomic group. The number of surveyed genomes in a taxonomic group is listed in parentheses. The shades of gray represent the proportion of these genomes in which the RcGTA homologs are found (see figure inset). Genomic regions were visualized using R package genoplotR (Guy et al. 2010).

Figure 3

Adjacency of the structural RcGTA homologs detected in α-proteobacterial genomes. The homologs were grouped into 474 genomic regions that contain between one and seventeen RcGTA homologs (shown on the X axis; see **Methods** for details on how the regions were identified). The variation of the observed cluster sizes is shown for each taxonomic group (arranged on Y axis) with at least one detected RcGTA homolog. The diameter of each circle is scaled with respect to the number of genomes (see inset for scale). The total number of genomes in each size category is shown in parentheses on the X-axis labels. The majority of clusters (245 out of 474, or 52%) contain at most two genes, and only 91 (19%) have nine or more RcGTA homologs. Adjacency of the structural RcGTA homologs detected in genomes across few other bacterial taxonomic groups is shown in **Supplementary Figure S2**.

Figure 4

Difference in GC content between clusters of RcGTA structural gene homologs and their host chromosome. The relative difference in GC content is calculated as $(GC_{GTA}-GC_{host})/GC_{host}$ (Y axis), and the data is presented by the number of RcGTA structural homologs found in a cluster (X axis). In the box-and-whisker plots the horizontal line marks the median; the boxes extend from the 25th to 75th percentile; the whiskers encompass values at most 1.5 times away from the 25th and 75th percentile range, and any value outside of the range is shown as a dot. The vertical dashed line separates two groups of clusters: ≤ 8 genes, or small clusters (SC, in blue) and ≥9 genes, or large clusters (LC, in orange). The inset depicts the combined data from all small and large clusters.

Figure 5

Distribution of RcGTA homologs in α-proteobacteria. The phylogenetic tree is a schematic version of the α-proteobacterial reference phylogeny (see **Methods** for reconstruction details), in which branches are collapsed at the taxonomic order level according to the NCBI Taxonomy database (NCBI Resource Coordinators 2017). The number of taxa in each collapsed clade is shown in parentheses. The tree is rooted using eight taxa from β-, γ- and δ-proteobacteria, which are collapsed into a clade labeled as "outgroup". The non-collapsed version of this tree is provided in **Supplementary Figure S3**. The nodes with at least 60% bootstrap support are labeled with a black circle. Bars associated with each clade show the relative proportion of genomes that contain at least one large cluster (orange), only small cluster(s) (blue), or no detectable RcGTA homologs at all (gray). Nodes 1 and 2 mark the last common ancestor of six taxonomic groups that contain large clusters and the last common ancestor of α-proteobacteria, respectively. These nodes define Clades 1 and 2 discussed in the text. Twenty-three of 150

genomes within Clade 1 and 32 out of 105 genomes outside of Clade 1 have no detectable RcGTA homologs. While relationships among the α-proteobacterial orders remain debated (Ferla et al. 2013; Gupta & Mok 2007; Lee et al. 2005; Luo 2014; Thrash et al. 2011; Williams et al. 2007), the discussed alternatives do not affect the inferences of this study. Scale bar, substitutions per site.

Figure 6

Comparison of the phylogenetic history of large clusters (right) to the reference α-proteobacterial phylogeny (left). Phylogenetic history of large clusters was reconstructed from the concatenated alignment of individual LC genes (LC-locus alignment), while the reference tree was reconstructed from the concatenated alignment of 99 conserved α-proteobacterial genes (see **Methods** for details). For each branch of the reference tree, the strength of its support on LC-locus tree was measured using an Internode Certainty (IC) value (Salichos et al. 2014), which reflects how many highly-supported bipartitions in 100 bootstrap trees of the LC-locus alignment support or conflict the reference tree branch. The branches of the reference tree are color-coded according to the strength of conflict categories: "strongly conflicting" (-1.0 ≤ IC ≤ -0.7), "moderately conflicting" (-0.7 < IC < 0.7) and "not conflicting" (0.7 ≤ IC ≤ 1.0). The overall number of branches with strongly conflicting IC values are shown as numbers (in pink) for "deep" and "shallow" branches, as demarcated by a vertical dashed line. Fourteen of the 15 strong conflicts at shallow branches occur within genera, and five of the six strong conflicts at deep branches are due to the different position of *Methylobacterium nodulans* ORS 2060. IC values for all branches are shown in **Supplementary Figure S7.** The phylogenetic tree on the left is rooted with the same outgroup as in **Supplementary Figure S3**, while the phylogenetic tree on the right should be considered unrooted. Nodes with bootstrap support values ≥80%

and between 60 and 80% are marked with closed and open circles, respectively. Nodes with bootstrap support values of <60% are unlabeled. Underlined taxa names represent four non-α-proteobacterial genomes that contain RcGTA-like large cluster (see also **Figures S6** and **S9**). Taxa names in brackets represent lineages that branch within a taxonomic order different from the one designated by the NCBI Taxonomy database (NCBI Resource Coordinators 2017). Scale bar, substitutions per site. The tree heights (*i.e.* the sum of all branch lengths of a phylogenetic tree) of the LC-locus and reference phylogenies are 31.19 and 19.39 substitutions per site, respectively, implying that the LC locus evolves approximately 1.6 times faster than the genomic regions that comprise conserved 99 genes.

Supplementary Data

SupplementaryFigures.pdf: Supplementary Figures 1-9

SupplementaryTables.xlsx: Supplementary Tables 1-5

Supplementary Figure Legends

Supplementary Figure S1

Compatibility of the evolutionary histories of the LC-locus and of individual LC genes. The sites of the LC-locus alignment are arranged along the X-axis, with the dashed red lines demarcating the alignment boundaries of the individual RcGTA-like genes (labeled with RcGTA gene names, g1 through g15; see **Supplementary Table S4**). For each alignment site, the Y-axis shows the phylogenetic distance between the optimal placement of a taxon in a phylogeny

reconstructed from a 100 amino-acid window that surrounds the site and in the LC-locus phylogeny, averaged across all sliding windows that contain the site. The Y-axis values averaged across all taxa and all sites within a gene is shown in parentheses on the X-axis. For 15 out of 17 genes, only 2-4 nodes separate the optimal taxon position in the LC-locus and gene phylogeny. The inflated distances for *g1* and *g3.5* are likely because only 15 and 21 of 95 LCs, respectively, have a homolog of these genes and the SSPB analysis is highly sensitive to missing data (Berger et al. 2011).

Supplementary Figure S2

Adjacency of the RcGTA structural homologs detected in genomes of (a) domain Bacteria, (b) phylum Proteobacteria, and (c) class γ-proteobacteria. For each panel, the variation of the observed cluster sizes (from 1 to 17 genes, arranged on the X-axis) is shown per taxonomic group (arranged on Y axis) with at least one detected RcGTA homolog. The diameter of each circle is scaled with respect to the number of genomes (same scale for all panels; see legend at the bottom of the **panel c**). The total number of genomes in each size category is shown in parentheses on the X-axis labels. Across bacteria, the clusters with at least nine RcGTA homologs are found predominantly in α-proteobacteria; the exceptions from other taxonomic groups are shown in orange.

Supplementary Figure S3

Distribution of RcGTA structural cluster homologs across α-proteobacterial genomes. Presence/absence and gene composition of RcGTA-like regions within each genome is mapped onto a maximum likelihood phylogeny that relates the 255 α-proteobacteria. The RcGTA homologs found on main replicons are shown in squares, and those found on plasmids or secondary replicons are denoted by circles. The symbols are color-coded according to the

cluster size (blue/orange), and presence of putatively pseudogenized RcGTA homologs (gray/black) and viral genes (red) within flanking regions (see **Supplementary Figures S5** and **S6**). Symbols outlined in red refer to RcGTA-like regions that overlap with PhiSpy-predicted prophages (Akhter et al. 2012). Taxa names are color-coded based on cluster size (blue/orange) or the absence of detectable structural homologs (black). Taxa labeled with an asterisk (*) designate genomes that have only non-structural RcGTA homologs. The taxa labeled with "++" represent two genomes of same strain in the 255 α-proteobacterial genome set; the corresponding cluster composition in the 2nd genome is shown in brackets. Labels to the right of the phylogenetic tree designate taxonomic groups according to the NCBI Taxonomy database (NCBI Resource Coordinators 2017). Taxon name in brackets represents lineage that branch within a taxonomic order different from the one designated by the NCBI Taxonomy database. Maximum likelihood phylogeny for α-proteobacteria was reconstructed using the concatenation of 99 protein-coding gene families that are present in at least 80% of 255 α-proteobacterial genomes. The tree is rooted using outgroup of eight taxa from β-, γ- and δ-proteobacteria (*Escherichia coli* str K12 substr DH10B, *Vibrio vulnificus* YJ016, *Pseudomonas aeruginosa* PAO1, *Pasteurella multocida* subsp multocida str Pm70, *Xanthomonas axonopodis* pv citri str 306, *Ralstonia solanacearum* GMI1000, *Chromobacterium violaceum* ATCC 12472, *Geobacter sulfurreducens* PCA). The nodes with at least 60% bootstrap support are labeled with a black dot.

Supplementary Figure S4

Comparison of pairwise phylogenetic distances (PPD) between homologs of structural RcGTA-like genes found in large clusters (LC, orange), small clusters (SC, blue) and viruses (red). In these box-and-whisker plots, the horizontal line marks the median, the boxes extend from the 25th to 75th percentile, the whiskers encompass values at most 1.5 times away

from the 25th and 75th percentile range, and any value outside of whiskers' range is shown as a dot. Number of data points (homologs) is shown in parentheses above the corresponding plots. Statistical significance of the difference in PPDs was assessed using Wilcoxon test in pairwise comparisons of the three groups (LCs, SCs, viruses). The tests were carried out only when at least four homologs were available in both compared groups. In the majority of the performed pairwise comparisons, LC genes had significantly lower PPDs than their counterparts in SCs and viruses (p-values < 0.05; see **Supplementary Table S5** for the detailed test results).

Supplementary Figure S5

Gene neighborhoods of 382 small clusters detected in α-proteobacterial genomes. Each genomic region shows annotated ORFs as arrows, and includes not only the SC homologs, but also several genes that flank the cluster on both 5' and 3' ends. The number of the flanking gene varies, with a requirement of at least five consecutive genes that are not assigned to a POG category. The regions are drawn to scale. The ORFs that correspond to the RcGTA-like homologs are colored in orange, while genes without similarity to RcGTA genes are either colored in red, if they were assigned to a POG category (and hence presumed to be of viral origin), or color-coded based on the abundance of the homologs in 255 α-proteobacterial genomes (see inset for color assignments). Incomplete or unannotated ORFs with significant nucleotide similarity to the RcGTA homologs are presumed to be putative pseudogenes and are shown in black. Thirty one of the 382 detected SCs contained 36 such putative pseudogenes, only three of which were found in SCs outside of Clade 1. The genomic regions are mapped onto the phylogenetic tree of SC-containing α-proteobacterial genomes reconstructed from the alignment of 99 core α-proteobacterial genes (see **Methods** for details), on which the nodes with ≥ 60% bootstrap support are marked with black circles. Names of taxa whose genomes also contain large clusters (see **Supplementary Figure S6**) are colored in orange, while names

of taxa whose genomes contain only small clusters are colored in blue. One hundred ninety nine out of the 382 SCs are found in taxa outside of Clade 1. Phylogenetic tree scale bar, substitutions per site. Genomic regions were visualized using R package genoplotR (Guy et al. 2010).

Supplementary Figure S6

Gene neighborhoods of 91 large clusters (LCs) found in α-proteobacterial genomes and 4 large clusters detected in four genomes outside of α-proteobacteria. Each genomic region shows annotated ORFs as arrows, and includes not only the LC homologs, but also several genes that flank the cluster on both 5' and 3' ends. The number of the flanking gene varies, with a requirement of at least five consecutive genes that are not assigned to a POG category. The regions are drawn to scale. Incomplete or unannotated ORFs with significant nucleotide similarity to the RcGTA homologs are presumed to be putative pseudogenes and are shown in black. The ORFs that correspond to the RcGTA-like homologs are colored in orange. Genes without similarity to the RcGTA genes are either colored in red, if they were assigned to a POG category (and hence presumed to be of viral origin), or color-coded based on the abundance of the homologs in 255 α-proteobacterial genomes (see inset for color assignments). Most LCs are flanked by conserved α-proteobacterial genes, and only 7 of 91 α-proteobacterial LCs have gene arrangements different from the RcGTA structural cluster. Thirty-six out of 91 α-proteobacterial LCs contain 67 putative pseudogenes. The genomic regions are mapped onto the phylogenetic tree that relates the 95 detected LCs, on which five copies of non-identical LCs found in *Methylobacterium nodulans* ORS 2060 are shown as individual taxa. The names of four taxa outside of α-proteobacteria are underlined. The phylogenetic tree was reconstructed from the alignment of concatenated RcGTA structural homologs, on which the nodes with ≥ 60%

bootstrap support are marked with black squares. Phylogenetic tree scale bar, substitutions per site. Genomic regions were visualized using R package genoplotR (Guy et al. 2010).

Supplementary Figure S7

Incongruence between the reference and LC-locus phylogenies. The depicted cladogram represents branching order of the reference phylogenetic tree shown on the left panel of the **Figure 6.** Background color of taxa labels correspond to the taxonomic orders; the same color scheme is used in **Figure 6**. The values above branches denote the rounded Internode Certainty (IC) values. Branches are colored based on the strength of conflict, which is classified into three categories: "strongly conflicting" (-1.0 ≤ IC ≤ -0.7), "moderately conflicting" (-0.7 < IC < 0.7) and "not conflicting" (0.7 ≤ IC ≤ 1.0); the same color scheme is used in **Figure 6**. A vertical dashed line divides branches of the tree into "deep" and "shallow" set, as in **Figure 6**.

Supplementary Figure S8

Phylogenetic trees of three genes that flank RcGTA-like clusters of *Scytonema millei* and *Pseudomonas bauzanensis*. All α-proteobacterial homologs of these genes that flank LCs in α-proteobacteria are also included. Taxa labels are colored by taxonomic affiliation: α-proteobacteria (black), cyanobacteria (green), and γ-proteobacteria (blue). The trees are rooted with cyanobacterial and γ-proteobacterial taxa that do not contain LCs, but are closely related to *Scytonema millei* and *Pseudomonas bauzanensis*. Bipartitions with bootstrap support ≥ 60% are labeled with black circles.

Supplementary Figure S9

Conservation of genomic regions that flank RcGTA-like large clusters, two operons of housekeeping genes and a transposable element from IS3/IS911 family as a function of evolutionary distance. Flanking regions are defined as 40 ORFs upstream (left panel) and downstream (right panel) of the examined loci in LC-containing α-proteobacterial genomes. Each dot represents a two-genome comparison, in which the proportion of common homologs among the 40 ORFs (Y axis) is plotted against the phylogenetic distance between the 16S rRNA genes of the two genomes (X axis). The model of gene order conservation (similar to model 3 in Rocha [2006]) was fitted into the data using non-linear regression (blue line). The estimates of the probabilities (*p*) of 40 genes to be found in the same region in consecutive generations are shown on the graphs. The model could not be fit for the transposable element data.

Supplementary Table Captions

Supplementary Table S1

List of 255 α-proteobacterial genomes used in the study.

Supplementary Table S2

List of 99 genes used to reconstruct α-proteobacterial reference phylogeny.

Supplementary Table S3

Relative Tree Certainty All (TCA) values for comparisons between the phylogenies reconstructed from the alignments of individual and concatenated large-cluster genes.

Supplementary Table S4

Functional annotations of genes in the RcGTA genome and their assignment to POG gene families.

Supplementary Table S5

Results of the pairwise Wilcoxon tests for comparisons of Pairwise Phylogenetic Distances' distributions of RcGTA-like genes found in large clusters, small clusters, and viruses.

References

Aberer, A. J., Krompass, D., & Stamatakis, A. (2013). 'Pruning rogue taxa improves phylogenetic accuracy: an efficient algorithm and web-service', *Systematic Biology*, 62/1: 162–6.

Akhter, S., Aziz, R. K., & Edwards, R. A. (2012). 'PhiSpy: a novel algorithm for finding prophages in bacterial genomes that combines similarity- and composition-based strategies', *Nucleic Acids Research*, 40/16: e126.

Al-Khedery, B., Lundgren, A. M., Stuen, S., et al. (2012). 'Structure of the type IV secretion system in different strains of *Anaplasma phagocytophilum*', *BMC Genomics*, 13: 678.

Alkhnbashi, O. S., Shah, S. A., Garrett, R. A., et al. (2016). 'Characterizing leader sequences of CRISPR loci', *Bioinformatics*, 32/17: i576–85.

Altschul, S. F., Madden, T. L., Schäffer, A. A., et al. (1997). 'Gapped BLAST and PSI-BLAST: a new generation of protein database search programs', *Nucleic Acids Research*, 25/17: 3389–402.

Andersson, J. O., & Andersson, S. G. (2001). 'Pseudogenes, junk DNA, and the dynamics of Rickettsia genomes', *Molecular Biology and Evolution*, 18/5: 829–39.

Bates, D. M., & Watts, D. G. (1988). 'Nonlinear regression analysis and its applications', John Wiley&Sons, Inc.

Berger, S. A., Krompass, D., & Stamatakis, A. (2011). 'Performance, accuracy, and web server for evolutionary placement of short sequence reads under maximum likelihood', *Systematic Biology*, 60/3: 291–302.

Berglund, E., Frank, A., Calteau, A., et al. (2009). 'run-off replication of host-adaptability genes

is associated with gene transfer agents in the genome of mouse-infecting *Bartonella grahamii*', *PLoS Genetics*, 5/7: e1000546.

Bertani, G. (1999). 'Transduction-like gene transfer in the methanogen *Methanococcus voltae*', *Journal of Bacteriology*, 181/10: 2992–3002.

Biers, E. J., Wang, K., Pennington, C., et al. (2008). 'Occurrence and expression of gene transfer agent genes in marine bacterioplankton', *Applied and Environmental Microbiology*, 74/10: 2933–9.

Bobay, L. M., Touchon, M., & Rocha, E. P. (2014). 'Pervasive domestication of defective prophages by bacteria', *Proceedings of the National Academy of Sciences of the United States of America*, 111/33: 12127-32.

Bobik, T. A., Lehman, B. P., & Yeates, T. O. (2015). 'Bacterial microcompartments: widespread prokaryotic organelles for isolation and optimization of metabolic pathways', *Molecular Microbiology*, 98/2: 193–207.

Böck, D., Medeiros, J. M., Tsao, H.-F., et al. (2017). 'In situ architecture, function, and evolution of a contractile injection system', *Science*, 357/6352: 713–7.

Borgeaud, S., Metzger, L. C., Scrignari, T., et al. (2015). 'Bacterial evolution. The type VI secretion system of *Vibrio cholerae* fosters horizontal gene transfer', *Science*, 347/6217: 63–7.

Brilli, M., Liò, P., Lacroix, V., et al. (2013). 'Short and long-term genome stability analysis of prokaryotic genomes', *BMC Genomics*, 14: 309.

Brimacombe, C. A., Ding, H., Johnson, J. A., et al. (2015). 'Homologues of genetic transformation DNA import genes are required for *Rhodobacter capsulatus* gene transfer agent recipient capability regulated by the response regulator CtrA', *Journal of Bacteriology*, 197/16: 2653–63.

Brimacombe, C., Stevens, A., Jun, D., et al. (2013). 'Quorum-sensing regulation of a capsular polysaccharide receptor for the *Rhodobacter capsulatus* gene transfer agent (RcGTA)', *Molecular Microbiology*, 87/4: 802–17.

Brindefalk, B., Ettema, T. J. G., Viklund, J., et al. (2011). 'A phylometagenomic exploration of oceanic alphaproteobacteria reveals mitochondrial relatives unrelated to the SAR11 clade', *PLoS One*, 6/9: e24457.

Canchaya, C., Proux, C., Fournous, G., et al. (2003). 'Prophage genomics', *Microbiology and Molecular Biology Reviews*, 67/2: 238–76.

Chandler, M., Fayet, O., Rousseau, P., et al. (2015). 'Copy-out-Paste-in transposition of IS911: A major transposition pathway', *Microbiology Spectrum*, 3/4. DOI: 10.1128/microbiolspec.MDNA3-0031-2014

Chen, F., Spano, A., Goodman, B. E., et al. (2009). 'Proteomic analysis and identification of the structural and regulatory proteins of the *Rhodobacter capsulatus* gene transfer agent', *Journal of Proteome Research*, 8/2: 967–73.

Chen, J. C., & Stephens, C. (2007). 'Bacterial cell cycle: completing the circuit', *Current Biology*,

17/6: R203–6.

Cobián Güemes, A. G., Youle, M., Cantú, V. A., et al. (2016). 'Viruses as Winners in the Game of Life', *Annual Review of Virology*, 3/1: 197–214.

Desantis, T., Hugenholtz, P., Larsen, N., et al. (2006). 'GreenGenes, a chimera-checked 16S rRNA gene database and workbench compatible with ARB', *Applied and Environmental Microbiology*, 72/7: 5069–72.

Díaz-Muñoz, S. L. (2017). 'Viral coinfection is shaped by host ecology and virus-virus interactions across diverse microbial taxa and environments', *Virus Evolution*, 3/1: vex011.

van Dongen, S. M. (2000). *Graph Clustering by Flow Simulation*. Ph.D. thesis, University of Utrecht.

Drake, J. W. (1999). 'The distribution of rates of spontaneous mutation over viruses, prokaryotes, and eukaryotes', *Annals of the New York Academy of Sciences*, 870: 100–7.

Edgar, R. (2004). 'MUSCLE: a multiple sequence alignment method with reduced time and space complexity', *BMC Bioinformatics*, 5: 113.

Edgar, R. (2007). 'PILER-CR: fast and accurate identification of CRISPR repeats', *BMC Bioinformatics*, 8: 18.

Ferla, M., Thrash, J. C., Giovannoni, S., et al. (2013). 'New rRNA gene-based phylogenies of the alphaproteobacteria provide perspective on major groups, mitochondrial ancestry and phylogenetic instability', *PLoS One*, 8/12: e83383.

Fogg, P. C., Westbye, A., & Beatty, J. T. (2012). 'One for all or all for one: heterogeneous expression and host cell lysis are key to gene transfer agent activity in *Rhodobacter capsulatus*', *PLoS One*, 7/8: e43772.

Frost, L., Leplae, R., Summers, A., et al. (2005). 'Mobile genetic elements: the agents of open source evolution', *Nature Reviews Microbiology*, 3/9: 722–32.

Gupta, R. S., & Mok, A. (2007). 'Phylogenomics and signature proteins for the alphaproteobacteria and its main groups', *BMC Microbiology*, 7: 106.

Guy, L., Kultima, J. R., & Andersson, S. G. E. (2010). 'genoPlotR: comparative gene and genome visualization in R', *Bioinformatics* , 26/18: 2334–5.

Guy, L., Nystedt, B., Toft, C., et al. (2013). 'A gene transfer agent and a dynamic repertoire of secretion systems hold the keys to the explosive radiation of the emerging pathogen Bartonella', *PLoS Genetics*, 9/3: e1003393.

Hershberg, R., & Petrov, D. A. (2010). 'Evidence that mutation is universally biased towards AT in bacteria', *PLoS Genetics*, 6/9: e1001115.

He, Z., Zhang, H., Gao, S., et al. (2016). 'Evolview v2: an online visualization and management tool for customized and annotated phylogenetic trees', *Nucleic Acids Research*, 44/W1: W236–41.

Hildebrand, F., Meyer, A., & Eyre-Walker, A. (2010). 'Evidence of selection upon genomic GC-

content in bacteria', *PLoS Genetics*, 6/9: e1001107.

Huang, S., Zhang, Y., Chen, F., et al. (2011). 'Complete genome sequence of a marine roseophage provides evidence into the evolution of gene transfer agents in alphaproteobacteria', *Virology Journal*, 8: 124.

Humphrey, S. B., Stanton, T. B., Jensen, N. S., et al. (1997). 'Purification and characterization of VSH-1, a generalized transducing bacteriophage of *Serpulina hyodysenteriae*', *Journal of Bacteriology*, 179/2: 323–9.

Hynes, A. P., Mercer, R. G., Watton, D., et al. (2012). 'DNA packaging bias and differential expression of gene transfer agent genes within a population during production and release of the *Rhodobacter capsulatus* gene transfer agent, RcGTA', *Molecular Microbiology*, 85/2: 314–25.

Hynes, A. P., Shakya, M., Mercer, R. G., et al. (2016). 'Functional and evolutionary characterization of a gene transfer agent's multilocus "genome"', *Molecular Biology and Evolution*, 33/10: 2530–43.

Iranzo, J., Krupovic, M., & Koonin, E. V. (2016). 'The double-stranded DNA virosphere as a modular hierarchical network of gene sharing', *mBio*, 7/4, e00978-16.

Iranzo, J., Krupovic, M., & Koonin, E. V. (2017). 'A network perspective on the virus world', *Communicative & Integrative Biology*, 10/2: e1296614.

Juhas, M., van der Meer, J. R., Gaillard, M., et al. (2009). 'Genomic islands: tools of bacterial horizontal gene transfer and evolution', *FEMS Microbiology Reviews*, 33/2: 376–93.

Ju, K.-S., Gao, J., Doroghazi, J. R., et al. (2015). 'Discovery of phosphonic acid natural products by mining the genomes of 10,000 actinomycetes', *Proceedings of the National Academy of Sciences of the United States of America*, 112/39: 12175–80.

Knoll, A. H. (2014). 'Paleobiological perspectives on early eukaryotic evolution', *Cold Spring Harbor Perspectives in Biology*, 6: a016121

Koonin, E., Senkevich, T., & Dolja, V. V. (2006). 'The ancient virus world and evolution of cells', *Biology Direct*, 1: 29.

Koonin, E. V. (2016). 'Horizontal gene transfer: essentiality and evolvability in prokaryotes, and roles in evolutionary transitions', *F1000Research*, 5: 1805.

Kristensen, D. M., Waller, A. S., Yamada, T., et al. (2013). 'Orthologous gene clusters and taxon signature genes for viruses of prokaryotes', *Journal of Bacteriology*, 195/5: 941–50.

Krupovic, M., & Koonin, E. V. (2017). 'Multiple origins of viral capsid proteins from cellular ancestors', *Proceedings of the National Academy of Sciences of the United States of America*, 114/12: E2401–10.

Kuchinski, K. S., Brimacombe, C. A., Westbye, A. B., et al. (2016). 'The SOS response master regulator LexA regulates the Gene Transfer Agent of *Rhodobacter capsulatus* and represses transcription of the signal transduction protein CckA', *Journal of Bacteriology*, 198/7: 1137–48.

Lang, A. S., & Beatty, J. T. (2000). 'Genetic analysis of a bacterial genetic exchange element: the gene transfer agent of *Rhodobacter capsulatus*', *Proceedings of the National Academy of Sciences of the United States of America*, 97/2: 859–64.

Lang, A. S., & Beatty, J. T. (2007). 'Importance of widespread gene transfer agent genes in alpha-proteobacteria', *Trends in Microbiology*, 15/2: 54–62.

Lang, A. S., Taylor, T., & Beatty, J. T. (2002). 'Evolutionary implications of phylogenetic analyses of the gene transfer agent (GTA) of *Rhodobacter capsulatus*', *Journal of Molecular Evolution*, 55/5: 534–43.

Lang, A. S., Westbye, A. B., & Beatty, J. T. (2017). 'The distribution, evolution, and roles of gene transfer agents in prokaryotic genetic exchange', *Annual Review of Virology*, ePub ahead of print. DOI: 10.1146/annurev-virology-101416-041624

Lang, A. S., Zhaxybayeva, O., & Beatty, J. T. (2012). 'Gene transfer agents: phage-like elements of genetic exchange', *Nature Reviews Microbiology*, 10/7: 472–82.

Lassalle, F., Périan, S., Bataillon, T., et al. (2015). 'GC-content evolution in bacterial genomes: the biased gene conversion hypothesis expands', *PLoS Genetics*, 11/2: e1004941.

Lawrence, J. G., Hendrix, R. W., & Casjens, S. (2001). 'Where are the pseudogenes in bacterial genomes?', *Trends in Microbiology*, 9/11: 535–40.

Lee, K. B., Liu, C. T., Anzai, Y., et al. (2005). 'The hierarchical system of the "Alphaproteobacteria": description of Hyphomonadaceae fam. nov., Xanthobacteraceae fam. nov. and Erythrobacteraceae fam. nov', *International Journal of Systematic and Evolutionary Microbiology*, 55/Pt 5: 1907–19.

Le, S. Q., & Gascuel, O. (2008). 'An improved general amino acid replacement matrix', *Molecular Biology and Evolution*, 25/7: 1307–20.

Leung, M., Brimacombe, C., Spiegelman, G. B., et al. (2012). 'The GtaR protein negatively regulates transcription of the gtaRI operon and modulates gene transfer agent (RcGTA) expression in *Rhodobacter capsulatus*', *Molecular Microbiology*, 83/4: 759–74.

Leung, M., Florizone, S., Taylor, T., et al. (2010). 'The gene transfer agent of *Rhodobacter capsulatus*', *Advances in Experimental Medicine and Biology*, 675: 253–64.

Li, L. (2003). 'OrthoMCL: Identification of ortholog groups for eukaryotic genomes', *Genome research*, 13/9: 2178–89.

Luo, H. (2014). 'Evolutionary origin of a streamlined marine bacterioplankton lineage', *The ISME Journal*, 9/6: 1423–33.

Luo, H., Csuros, M., Hughes, A., et al. (2013). 'Evolution of divergent life history strategies in marine alphaproteobacteria', *mBio*, 4/4: e00373–13.

Makarova, K. S., Wolf, Y. I., Alkhnbashi, O. S., et al. (2015). 'An updated evolutionary classification of CRISPR-Cas systems', *Nature Reviews Microbiology*, 13/11: 722–36.

Mann, T. H., Seth Childers, W., Blair, J. A., et al. (2016). 'A cell cycle kinase with tandem sensory PAS domains integrates cell fate cues', *Nature Communications*, 7: 11454.

Marrs, B. (1974). 'Genetic recombination in *Rhodopseudomonas capsulata*', *Proceedings of the National Academy of Sciences of the United States of America*, 71/3: 971–3.

McDaniel, L., Young, E., Delaney, J., et al. (2010). 'High frequency of horizontal gene transfer in the oceans', *Science*, 330/6000: 50.

McDaniel, L., Young, E., Ritchie, K., et al. (2012). 'Environmental factors influencing gene transfer agent (GTA) mediated transduction in the subtropical ocean', *PLoS One*, 7/8: e43506.

McHugh, C. A., Fontana, J., Nemecek, D., et al. (2014). 'A virus capsid-like nanocompartment that stores iron and protects bacteria from oxidative stress', *The EMBO Journal*, 33/17: 1896–911.

Mercer, R. G., & Lang, A. S. (2014). 'Identification of a predicted partner-switching system that affects production of the gene transfer agent RcGTA and stationary phase viability in *Rhodobacter capsulatus*', *BMC Microbiology*, 14: 71.

Mira, A., Ochman, H., & Moran, N. A. (2001). 'Deletional bias and the evolution of bacterial genomes', *Trends in Genetics*, 17/10: 589–96.

Nagao, N., Yamamoto, J., Komatsu, H., et al. (2015). 'The gene transfer agent-like particle of the marine phototrophic bacterium *Rhodovulum sulfidophilum*', *Biochemistry and Biophysics Reports*, 4: 369–74.

NCBI Resource Coordinators (2017). 'Database Resources of the National Center for Biotechnology Information', *Nucleic Acids Research*, 45/D1: D12–7.

Paterson, S., Vogwill, T., Buckling, A., et al. (2010). 'Antagonistic coevolution accelerates molecular evolution', *Nature*, 464/7286: 275–8.

Price, M. N., Dehal, P. S., & Arkin, A. P. (2010). 'FastTree 2--approximately maximum-likelihood trees for large alignments', *PloS One*, 5/3: e9490.

Rapp, B. J., & Wall, J. D. (1987). 'Genetic transfer in *Desulfovibrio desulfuricans*', *Proceedings of the National Academy of Sciences of the United States of America*, 84/24: 9128–30.

Redfield, R. J. (2001). 'Do bacteria have sex?', *Nature Reviews Genetics*, 2/8: 634–9.

Richards, T. A., & Archibald, J. M. (2011). 'Cell evolution: gene transfer agents and the origin of mitochondria', *Current Biology*, 21/3: R112–4.

Rocha, E. P. C. (2006). 'Inference and analysis of the relative stability of bacterial chromosomes', *Molecular Biology and Evolution*, 23/3: 513–22.

Rocha, E. P. C., & Danchin, A. (2002). 'Base composition bias might result from competition for metabolic resources', *Trends in Genetics*, 18/6: 291–4.

Rocha, E. P. C., & Feil, E. J. (2010). 'Mutational patterns cannot explain genome composition: Are there any neutral sites in the genomes of bacteria?', *PLoS Genetics*, 6/9: e1001104.

Rodriguez-Valera, F., Martin-Cuadrado, A.-B., & López-Pérez, M. (2016). 'Flexible genomic islands as drivers of genome evolution', *Current Opinion in Microbiology*, 31: 154–60.

Salichos, L., Stamatakis, A., & Rokas, A. (2014). 'Novel information theory-based measures for quantifying incongruence among phylogenetic trees', *Molecular Biology and Evolution*, 31/5: 1261–71.

Sarris, P. F., Ladoukakis, E. D., Panopoulos, N. J., et al. (2014). 'A phage tail-derived element with wide distribution among both prokaryotic domains: a comparative genomic and phylogenetic study', *Genome Biology and Evolution*, 6/7: 1739–47.

Schaefer, A. L., Taylor, T., Beatty, J. T., et al. (2002). 'Long-chain acyl-homoserine lactone quorum-sensing regulation of *Rhodobacter capsulatus* gene transfer agent production', *Journal of Bacteriology*, 184/23: 6515–21.

Schloss, P., Westcott, S., Ryabin, T., et al. (2009). 'Introducing mothur: Open-source, platform-independent, community-supported software for describing and comparing microbial communities', *Applied and Environmental Microbiology*, 75/23: 7537–41.

Sen, D., Chandrababunaidu, M. M., Singh, D., et al. (2015). 'Draft genome sequence of the terrestrial cyanobacterium *Scytonema millei* VB511283, Isolated from Eastern India', *Genome Announcements*, 3/2: e00009-15.

Shikuma, N. J., Pilhofer, M., Weiss, G. L., et al. (2014). 'Marine tubeworm metamorphosis induced by arrays of bacterial phage tail-like structures', *Science*, 343/6170: 529–33.

Smillie, C. S., Smith, M. B., Friedman, J., et al. (2011). 'Ecology drives a global network of gene exchange connecting the human microbiome', *Nature*, 480/7376: 241–4.

Solioz, M., & Marrs, B. (1977). 'The gene transfer agent of *Rhodopseudomonas capsulata*. Purification and characterization of its nucleic acid', *Archives of Biochemistry and Biophysics*, 181/1: 300–7.

Stamatakis, A. (2014). 'RAxML version 8: a tool for phylogenetic analysis and post-analysis of large phylogenies', *Bioinformatics* , 30/9: 1312–3.

Sutter, M., Boehringer, D., Gutmann, S., et al. (2008). 'Structural basis of enzyme encapsulation into a bacterial nanocompartment', *Nature Structural & Molecular Biology*, 15/9: 939–47.

Thrash, J., Boyd, A., Huggett, M., et al. (2011). 'Phylogenomic evidence for a common ancestor of mitochondria and the SAR11 clade', *Scientific Reports*, 1: 1–9.

Touchon, M., Bernheim, A., & Rocha, E. P. (2016). 'Genetic and life-history traits associated with the distribution of prophages in bacteria', *The ISME Journal, 10: 2744-2754*.

Touchon, M., Bobay, L.-M., & Rocha, E. P. C. (2014). 'The chromosomal accommodation and domestication of mobile genetic elements', *Current Opinion in Microbiology*, 22: 22–9.

Touchon, M., Moura de Sousa, J. A., & Rocha, E. P. (2017). 'Embracing the enemy: the diversification of microbial gene repertoires by phage-mediated horizontal gene transfer', *Current Opinion in Microbiology*, 38: 66–73.

Wang, X., Jin, D., Zhou, L., et al. (2014). 'Draft genome sequence of halotolerant polycyclic aromatic hydrocarbon-degrading *Pseudomonas bauzanensis* strain W13Z2', *Genome Announcements*, 2/5: e01049-14.

Wang, X., Kim, Y., Ma, Q., et al. (2010). ‘Cryptic prophages help bacteria cope with adverse environments’, *Nature Communications*, 1: 147.

Wang, Z., & Wu, M. (2015). ‘An integrated phylogenomic approach toward pinpointing the origin of mitochondria’, *Scientific Reports*, 5: 7949.

Westbye, A. B., Kuchinski, K., Yip, C. K., et al. (2015). ‘The gene transfer agent RcGTA contains head spikes needed for binding to the *Rhodobacter capsulatus* polysaccharide cell capsule’, *Journal of Molecular Biology,* 428 (2 Pt B): 477-91.

Westbye, A. B., Leung, M. M., Florizone, S. M., et al. (2013). ‘Phosphate concentration and the putative sensor kinase protein CckA modulate cell lysis and release of the *Rhodobacter capsulatus* gene transfer agent’, *Journal of Bacteriology*, 195/22: 5025–40.

Williams, K. P., Sobral, B. W., & Dickerman, A. W. (2007). ‘A robust species tree for the alphaproteobacteria’, *Journal of Bacteriology*, 189/13: 4578–86.

Yang, Z. (1994). ‘Maximum likelihood phylogenetic estimation from DNA sequences with variable rates over sites: approximate methods’, *Journal of Molecular Evolution*, 39/3: 306–14.

Zan, J., Heindl, J., Liu, Y., et al. (2013). ‘The CckA-ChpT-CtrA phosphorelay system is regulated by quorum sensing and controls flagellar motility in the marine sponge symbiont *Ruegeria* sp. KLH11’, *PLoS One*, 8/6: e66346.

Zhan, Y., Huang, S., Voget, S., et al. (2016). ‘A novel roseobacter phage possesses features of podoviruses, siphoviruses, prophages and gene transfer agents’, *Scientific Reports*, 6: 30372.

Zhaxybayeva, O., & Doolittle, W. F. (2011). ‘Lateral gene transfer’, *Current Biology*, 21/7: R242–6.

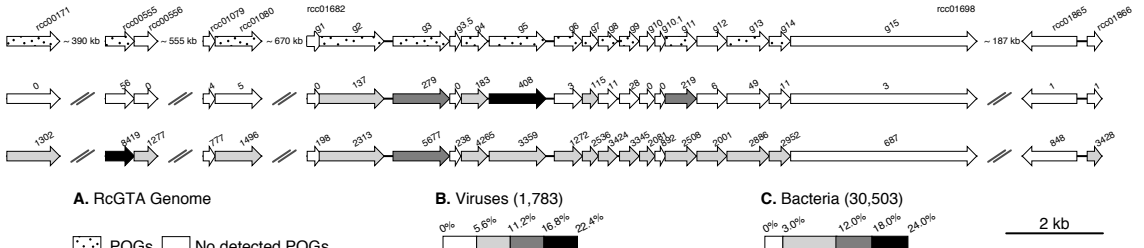
A.
B.
C.
rcc00171
~ 390 kb
rcc00555
rcc00556
~ 555 kb
rcc01079
rcc01080
~ 670 kb
rcc01682
91
92
93
93.5
94
95
96
97
98
99
910
910.1
911
912
913
914
915
rcc01698
~ 187 kb
rcc01865
rcc01866
0
56
0
4
5
0
137
279
0
183
408
3
115
11
28
0
0
219
6
49
11
3
1
1
1302
8419
1277
1777
1496
198
2313
5677
238
4265
3359
1272
2536
3424
3345
2081
2632
2508
2001
2886
2952
687
848
3428
A. RcGTA Genome
POGs
No detected POGs
B. Viruses (1,783)
0%
5.6%
11.2%
16.8%
22.4%
C. Bacteria (30,503)
0%
3.0%
12.0%
18.0%
24.0%
2 kb

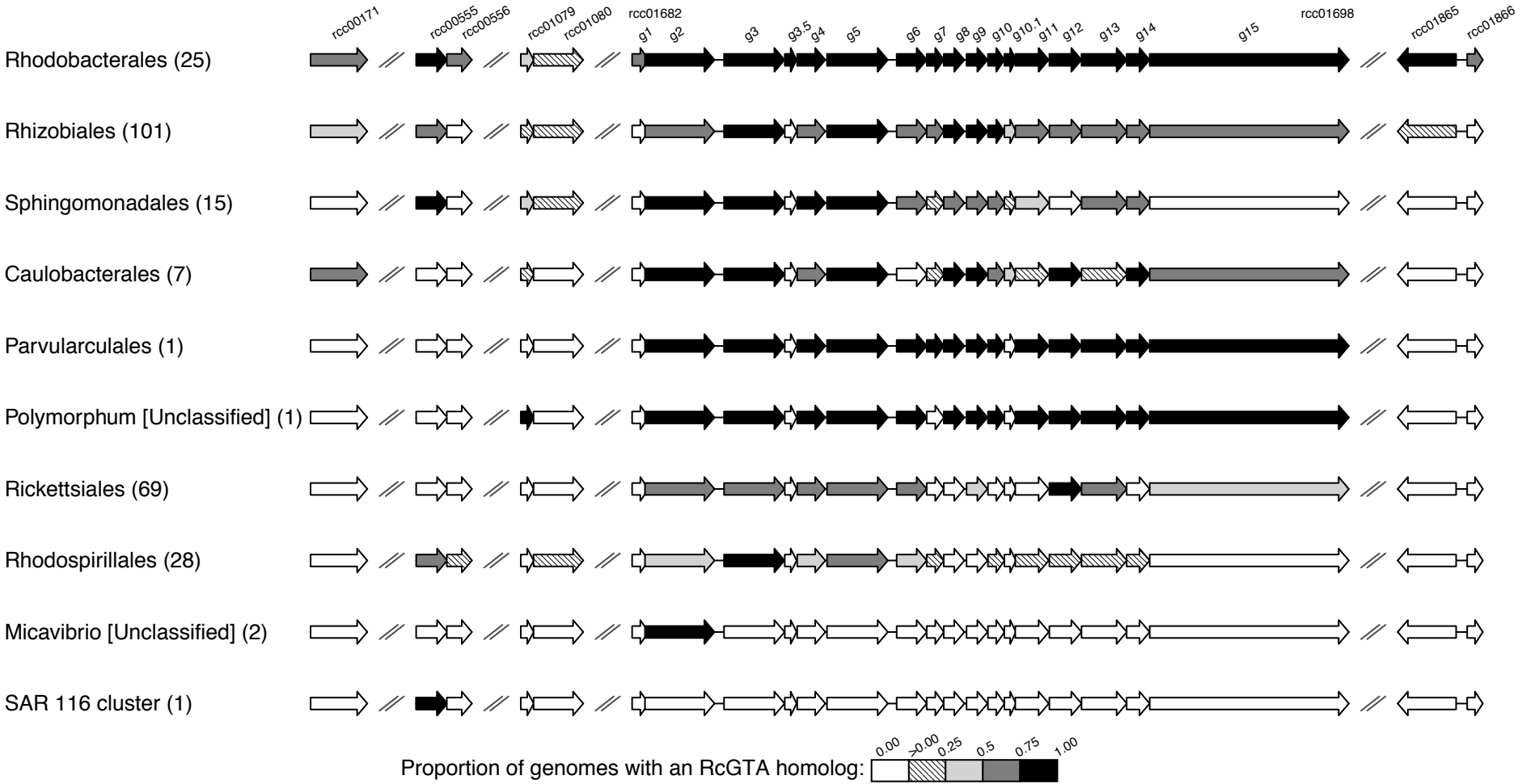
rcc00171
rcc00555
rcc00556
rcc01079
rcc01080
rcc01682
g1
g2
g3
g3.5
g4
g5
g6
g7
g8
g9
g10
g10.1
g11
g12
g13
g14
g15
rcc01698
rcc01865
rcc01866
Rhodobacterales (25)
Rhizobiales (101)
Sphingomonadales (15)
Caulobacterales (7)
Parvularculales (1)
Polymorphum [Unclassified] (1)
Rickettsiales (69)
Rhodospirillales (28)
Micavibrio [Unclassified] (2)
SAR 116 cluster (1)
Proportion of genomes with an RcGTA homolog:
0.00
>0.00
0.25
0.5
0.75
1.00

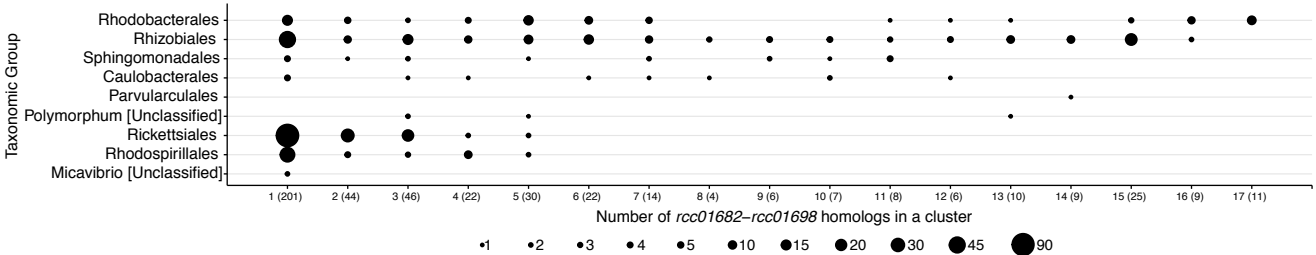
Taxonomic Group
Rhodobacterales
Rhizobiales
Sphingomonadales
Caulobacterales
Parvularculales
Polymorphum [Unclassified]
Rickettsiales
Rhodospirillales
Micavibrio [Unclassified]
1 (201)
2 (44)
3 (46)
4 (22)
5 (30)
6 (22)
7 (14)
8 (4)
9 (6)
10 (7)
11 (8)
12 (6)
13 (10)
14 (9)
15 (25)
16 (9)
17 (11)
Number of *rcc01682–rcc01698* homologs in a cluster
1
2
3
4
5
10
15
20
30
45
90

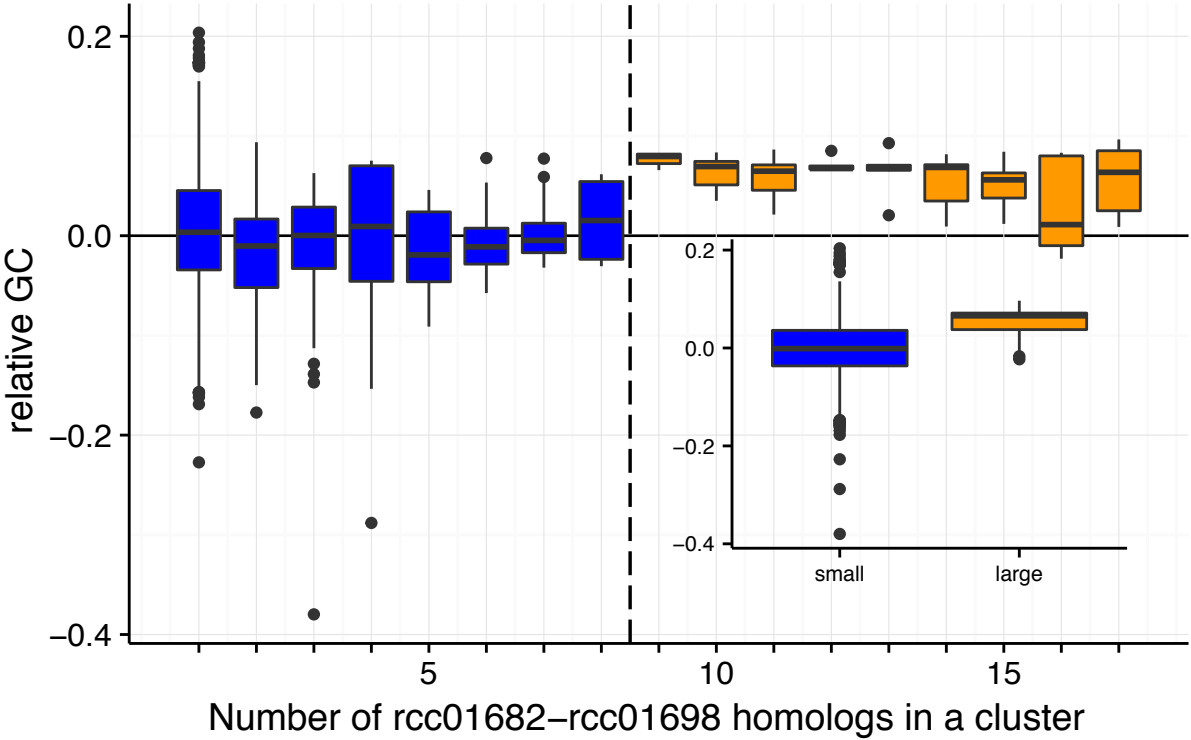
0.2
0.0
−0.2
−0.4
relative GC
5
10
15
Number of rcc01682−rcc01698 homologs in a cluster
0.2
0.0
−0.2
−0.4
small
large

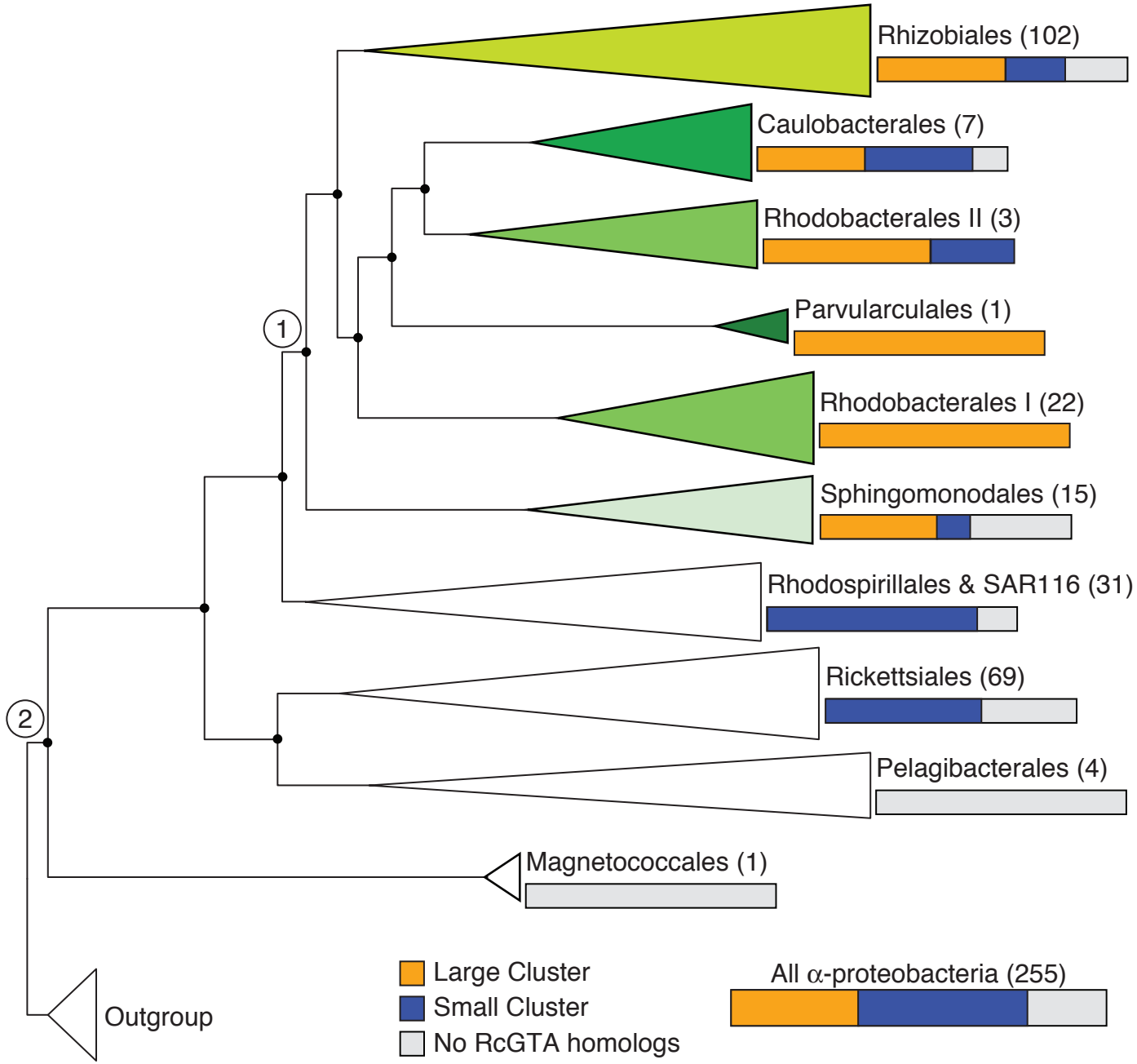
Rhizobiales (102)
Caulobacterales (7)
Rhodobacterales II (3)
Parvularculales (1)
Rhodobacterales I (22)
Sphingomonodales (15)
Rhodospirillales & SAR116 (31)
Rickettsiales (69)
Pelagibacterales (4)
Magnetococcales (1)
1
2
Outgroup
Large Cluster
Small Cluster
No RcGTA homologs
All α-proteobacteria (255)

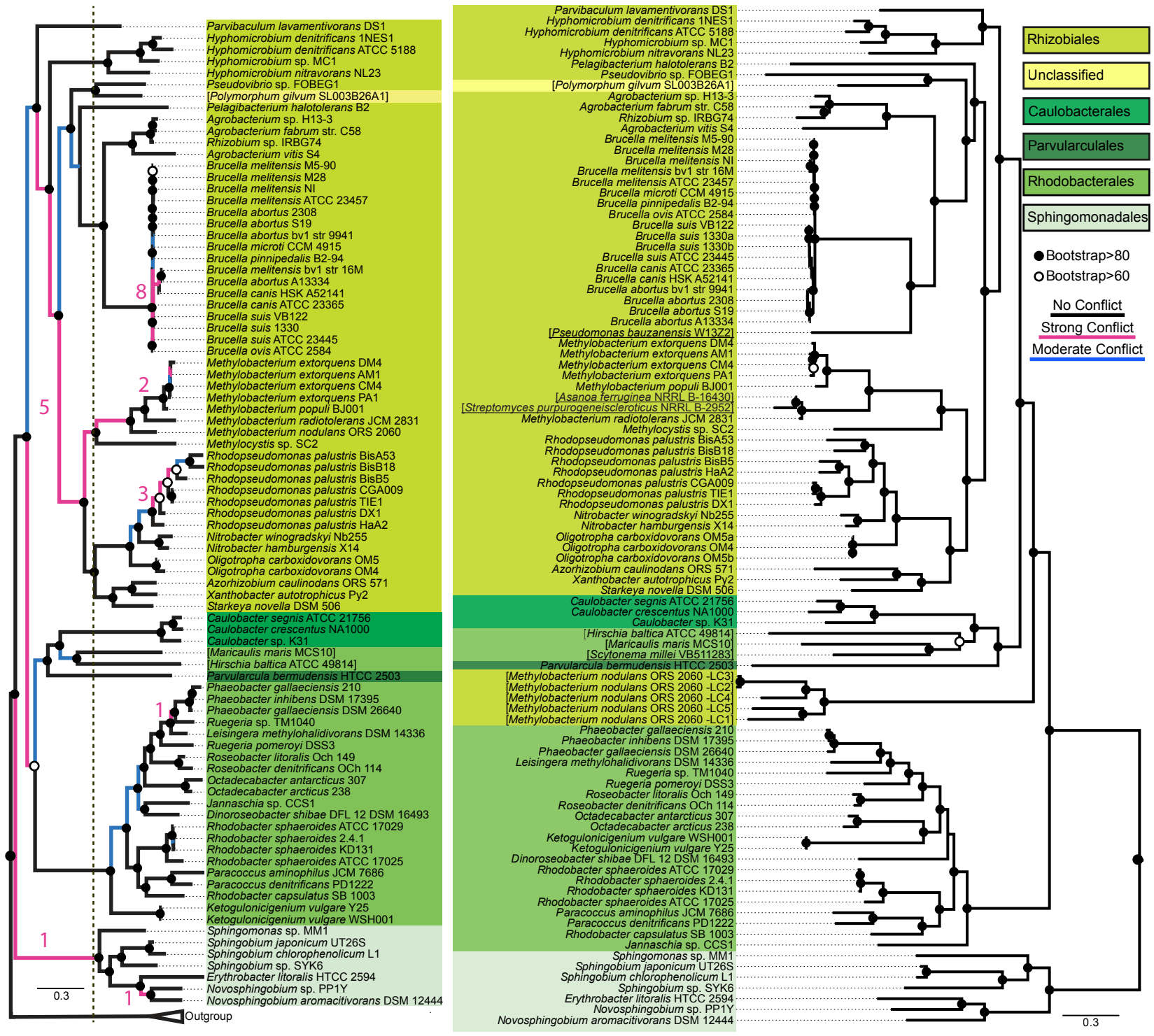
Parvibaculum lavamentivorans DS1
Hyphomicrobium denitrificans 1NES1
Hyphomicrobium denitrificans ATCC 5188
Hyphomicrobium sp. MC1
Hyphomicrobium nitravorans NL23
Pseudovibrio sp. FOBEG1
[Polymorphum gilvum SL003B26A1]
Pelagibacterium halotolerans B2
Agrobacterium sp. H13-3
Agrobacterium fabrum str. C58
Rhizobium sp. IRBG74
Agrobacterium vitis S4
Brucella melitensis M5-90
Brucella melitensis M28
Brucella melitensis NI
Brucella melitensis ATCC 23457
Brucella abortus 2308
Brucella abortus S19
Brucella abortus bv1 str 9941
Brucella microti CCM 4915
Brucella pinnipedalis B2-94
Brucella melitensis bv1 str 16M
Brucella abortus A13334
Brucella canis HSK A52141
Brucella canis ATCC 23365
Brucella suis VB122
Brucella suis 1330
Brucella suis ATCC 23445
Brucella ovis ATCC 2584
Methylobacterium extorquens DM4
Methylobacterium extorquens AM1
Methylobacterium extorquens CM4
Methylobacterium extorquens PA1
Methylobacterium populi BJ001
Methylobacterium radiotolerans JCM 2831
Methylobacterium nodulans ORS 2060
Methylocystis sp. SC2
Rhodopseudomonas palustris BisA53
Rhodopseudomonas palustris BisB18
Rhodopseudomonas palustris BisB5
Rhodopseudomonas palustris CGA009
Rhodopseudomonas palustris TIE1
Rhodopseudomonas palustris DX1
Rhodopseudomonas palustris HaA2
Nitrobacter winogradskyi Nb255
Nitrobacter hamburgensis X14
Oligotropha carboxidovorans OM5
Oligotropha carboxidovorans OM4
Azorhizobium caulinodans ORS 571
Xanthobacter autotrophicus Py2
Starkeya novella DSM 506
Caulobacter segnis ATCC 21756
Caulobacter crescentus NA1000
Caulobacter sp. K31
[Maricaulis maris MCS10]
[Hirschia baltica ATCC 49814]
Parvularcula bermudensis HTCC 2503
Phaeobacter gallaeciensis 210
Phaeobacter inhibens DSM 17395
Phaeobacter gallaeciensis DSM 26640
Ruegeria sp. TM1040
Leisingera methylohalidivorans DSM 14336
Ruegeria pomeroyi DSS3
Roseobacter litoralis Och 149
Roseobacter denitrificans OCh 114
Octadecabacter antarcticus 307
Octadecabacter arcticus 238
Jannaschia sp. CCS1
Dinoroseobacter shibae DFL 12 DSM 16493
Rhodobacter sphaeroides ATCC 17029
Rhodobacter sphaeroides 2.4.1
Rhodobacter sphaeroides KD131
Rhodobacter sphaeroides ATCC 17025
Paracoccus aminophilus JCM 7686
Paracoccus denitrificans PD1222
Rhodobacter capsulatus SB 1003
Ketogulonicigenium vulgare Y25
Ketogulonicigenium vulgare WSH001
Sphingomonas sp. MM1
Sphingobium japonicum UT26S
Sphingobium chlorophenolicum L1
Sphingobium sp. SYK6
Erythrobacter litoralis HTCC 2594
Novosphingobium sp. PP1Y
Novosphingobium aromacitivorans DSM 12444
Outgroup
8
2
5
3
1
1
1
0.3
[Pseudomonas bauzanensis W13Z2]
[Asanoa ferruginea NRRL B-16430]
[Streptomyces purpurogeneiscleroticus NRRL B-2952]
[Methylobacterium nodulans ORS 2060 -LC3]
[Methylobacterium nodulans ORS 2060 -LC2]
[Methylobacterium nodulans ORS 2060 -LC4]
[Methylobacterium nodulans ORS 2060 -LC5]
[Methylobacterium nodulans ORS 2060 -LC1]
Rhizobiales
Unclassified
Caulobacterales
Parvularculales
Rhodobacterales
Sphingomonadales
Bootstrap>80
Bootstrap>60
No Conflict
Strong Conflict
Moderate Conflict
0.3